Comparison of uniform and piecewise-uniform heatings when estimating thermal properties of high-conductivity materials

Giampaolo d'Alessandro, Filippo de Monte, Suelen Gasparin, Julien Berger

Comparison of uniform and piecewise-uniform heatings when estimating thermal properties of high-conductivity materials

G D'Alessandro[a,*], F de Monte[a], S Gasparin[b], J Berger[c]

[a] Department of Industrial and Information Engineering and Economics, University of L'Aquila, 67100 L'Aquila, Italy
[b] Cerema, BPE Research team, 44200 Nantes, France
[c] Laboratory of Engineering Sciences for the Environment (LaSIE), UMR 7356 CNRS, La Rochelle University, CNRS, 17000, La Rochelle, France

* Correspondig author: giampaolo.dalessandro@univaq.it

Abstract. A D-optimum criterion is applied to the three-layer apparatus used for simultaneously estimating thermal properties (for example, thermal conductivity and effusivity) through the plane source method. The objective is to perform a comparison between uniform heating and piecewise-uniform heating of high-conductivity solid samples. In particular, the latter case is modeled through a two-dimensional heat conduction problem in which a rectangular plate (i.e. the sample) is partially heated at the front boundary through a surface heat flux, while all the other boundaries are kept insulated. The optimal experiment is designed for different set-ups of the experimental apparatus (width of the heated region, number of sensors and their locations). The convergence and the computational efficiency of the estimation iterative procedure are the terms of the comparison, as well as the expected standard deviations of thermal conductivity and effusivity. The results indicate that the use of a piecewise-uniform heating is not completely beneficial for isotropic materials. In fact, if on one hand it may offer standard deviations reduced up to about 40%, on the other hand it would require an experiment about four times longer than that required by a uniform heating to ensure a good convergence of the estimation iterative procedure. Therefore, a major computational effort is required.

Keywords optimal experiment design, D-optimum criterion, uniform and partial heatings, transient heat conduction, thermal properties, uncertainty of the estimates

Nomenclature

$\underline{b}$	estimated parameter vector
C	volumetric heat capacity [J/(m^3°C)]
$\widetilde{C}^{+}_{ij}$	dimensionless coefficient of the $\underline{\tilde{X}}^{T}\,\underline{\tilde{X}}$ matrix, with $i, j = k, \varepsilon$
$H(\cdot)$	Heaviside function
h_L	heat transfer coefficient at the sample backside [W/(m^{2}K)]
k	thermal conductivity [W/(mK)]
L	thickness [m]
N	number of measurements

q''	time-dependent heat flux per unit area [W/m^2]
q_0''	uniform surface heat flux per unit area [W/m^2]
S	number of sensors
T	temperature [K]
T_{max}	maximum temperature reached during the experiment [K]
t	time [s]
t_h	heating time [s]
t_N	experiment time [s]
W	width of the rectangular domain [m]
W_0	width of the heated region [m]
X	scaled sensitivity coefficient [K]
$\underline{X}$	scaled sensitivity coefficient matrix [K]
x	space coordinate along the x-direction [m]
y	space coordinate along the y-direction [m]
$\tilde{y}_{i,s}$	dimensionless y-coordinate for the i-th sensor (i=1,2,3)
$\underline{Y}$	simulated temperature matrix [K]
Z	sensitivity coefficient
$\underline{Z}$	sensitivity coefficients matrix

Greek symbols

α	thermal diffusivity [m^2/s]
β_m	m-th dimensionless eigenvalue along the x-direction
γ	generic parameter, with $\gamma = k, \varepsilon$
Δ^+	determinant of the $\underline{\tilde{X}}^T \underline{\tilde{X}}$ matrix
ε	thermal effusivity [J/(m^{2}Ks$^{1/2}$)]
η_n	n-th dimensionless eigenvalue along the y-direction
σ	standard deviation
$\tilde{\sigma}_i^+$	dimensionless standard deviation, with i= k, ε
$\tilde{\tau}$	variable, $\tilde{\tau} = \tilde{t} - \tilde{t}_h$

Subscripts

h	heating
in	initial
m	counting integer for eigenvalues along the x-direction
max	maximum
n	counting integer for eigenvalues along the y-direction
opt	optimal
s	sensor location
$X22$	X22B10T0 case
$Y22$	Y22B00Gy5T0 case
$XY22$	X22By50Y22B00T0 case
xy	transient 2D component of the temperature solution

Superscripts

$(B5)$	temperature solution for finite heating period
~	dimensionless
T	transpose

1. Introduction

Transient methods to estimate the thermal properties of solid materials allow both thermal conductivity and volumetric heat capacity to be measured simultaneously [1-5]. When using these methods different experimental devices can be employed. In particular, some of them involve a nonuniform heating of the sample and are used for estimating the different, directional, thermal conductivities of orthotropic materials. Such nonuniform heating can be applied through both a partial heating [6-10] and a sinusoidal-in-space heating [11]. The former is applied when testing composites and orthotropic materials in general, while the latter is used when thermal properties of thin films are desired. Other experimental apparatuses are based on a uniform heating [2, 12] of the solid specimen which is suitable for the estimation of thermal conductivity, thermal effusivity (or volumetric heat capacity) of isotropic material, such as metals and plastic materials. Note that from an experimental point of view, thermal properties measurement of low conductivity materials requires to approximate an isothermal boundary condition (placing the sample in perfect thermal contact with a high-conductivity material), while an insulated boundary condition is more appropriate when testing metals, as they can be easily insulated having high thermal conductivity.

Among the transient methods, the plane source method [13, 14] for the estimation of thermal properties of high-conductivity solid materials is here of interest. In particular, the three-layer experimental apparatus used in such a case consists of a thin electrical heater sandwiched between two samples of the same material and thickness, having all the boundaries insulated. Depending upon the dimensions of the heater used to heat up the two samples, this apparatus may have two different experimental set-ups. In fact, the use of a heater having the same dimensions of the samples yields a uniform heating of both of them, while when using a smaller one, a piecewise-uniform (partial) heating is supplied. As known the latter set-up is usually used to estimate the directional thermal conductivities of orthotropic materials. However, the aim of the present work is to investigate whether a piecewise-uniform heating may offer some advantages, in terms of convergence and computational efficiency of the parameters estimation procedure, and also accuracy (standard deviations) of the obtained estimates, when estimating simultaneously the thermal properties of isotropic materials as compared to the uniform heating. This comparison is performed by designing the optimal experiment for both set-ups. Specifically, optimal experiment design allows as much of insights and information as possible to be obtained from the recorded temperature data. In fact, in parameter estimation problems it is of great concern that the measured temperatures are sensitive to the unknown parameters of interest in order to obtain reliable and good estimates for them. In other words, optimal experiment design may suggest the optimum sensors locations [10, 15, 16], the optimum heating and experiment times [13, 17, 18], the optimum geometrical sample configuration [9], and the optimum heat flux applied to the sample [9, 16] to obtain the greatest accuracy of the estimated parameters. Also it may provide insight about which quantities can be conveniently estimated. Several optimization criteria have been suggested, such as the D-optimum criteria based on the maximization of the Fisher matrix determinant [19, 20], the E-optimum criteria requiring the maximization of the minimum eigenvalue of the $\underline{X}^T\underline{X}$ matrix [9] and the A-optimum criteria based on the maximization of the trace of the same matrix [21]. Moreover and alternatively, researchers have also tried innovative approaches based on stochastic optimization algorithms [21], machine learning [22, 23] and convex relaxation strategy [24].

A D-optimum criterion, called Δ^+ criterion [19], is here used to design the optimal experiment aimed at estimating simultaneously thermal conductivity k and thermal effusivity ε (with $\varepsilon = \sqrt{kC}$) when using the plane source-based experimental apparatus for the two different set-ups (uniform and partial heating). It is worth to underline that all the results here derived are valid for isotropic materials only. Also, the Δ^+ criterion requires the maximization of the $\underline{\tilde{X}}^T\underline{\tilde{X}}$ determinant (with $\tilde{X}$ the dimensionless scaled sensitivity matrix) whose magnitude not only affects the convergence of the parameters estimation procedure, but also affects the covariance matrix of the estimated parameters and, therefore, their uncertainty. The magnitude of the Δ^+ determinant depends on the choice of the parameters to be estimated. In fact, the choice to estimate k and ε yields a determinant four times

greater than that obtained for the pair k and C. However, for the sake of brevity the proof of that is not discussed here. Moreover, as the optimization procedure stated above involves the sensitivity coefficients of temperature with respect to the properties of interest, the knowledge of the temperature field inside the sample is required for their computation.

For this purpose, the experimental apparatus is modeled by neglecting the thermal inertia of the heater, the surface contact resistance at the sample/heater interface and the heat loss at the sample backside through the insulating material. Note that a complete description of the apparatus including the inertia of the heater and the imperfect contact between heater and sample, when applying a uniform heating, can be found in references [18] and [13,14], respectively.

Therefore, the set-up related to a piecewise-uniform heating is investigated through a two-dimensional heat conduction problem involving a rectangular plate (representing the sample) partially heated at the front boundary through a surface heat flux, and having all its other boundaries insulated. Also, the heater is completely neglected as well as the heat loss at the sample backside. Furthermore, to take into account a finite heating duration, the exact analytical solution is determined by means of the superposition principle starting from a solution available in the literature [25]. After that, the sensitivity coefficients with respect to k and ε are computed through a finite difference scheme. Then, the optimal experiment is designed for different set-ups of the experimental apparatus that is, for different widths of the heated region and for a different number of sensors placed in several non-embedded locations at both the front side and backside of the sample. The Δ^+ determinant and the optimum experiment duration (which are strictly related to the convergence of the estimation procedure and to the computational efficiency of the same procedure, respectively) obtained when the sample is subject to a uniform or a partial heating are compared in both graphical and tabular form. In addition, for the best sensors configurations the related expected standard deviations of k and ε when applying a partial heating are computed and compared with those obtained under a uniform heating.

The paper is organized as follows. Once the problem is described (Section 2), the mathematical model is discussed in Section 3. The sensitivity coefficients are defined in Section 4, while in Section 5 the criterion used to design the optimal experiment and the computation of the standard deviations are treated. Lastly the results are shown and discussed in Section 6.

2. Description of the problem

The experimental apparatus used in the plane source method for thermal properties estimation of high-conductivity solid materials consists of a thin electrical heater sandwiched between two samples of the same material and thickness, which heat up the surface of both samples [13, 14]. In such a way the experimentalist can be sure that the heating power delivered by the heater is equally given to the two samples. Note that the same apparatus may be used to create both a uniform heating, when the heater covers the whole surface of the samples (figure 1a), and a partial heating when the heater covers partially the interface surface between the two samples (figure 1b).

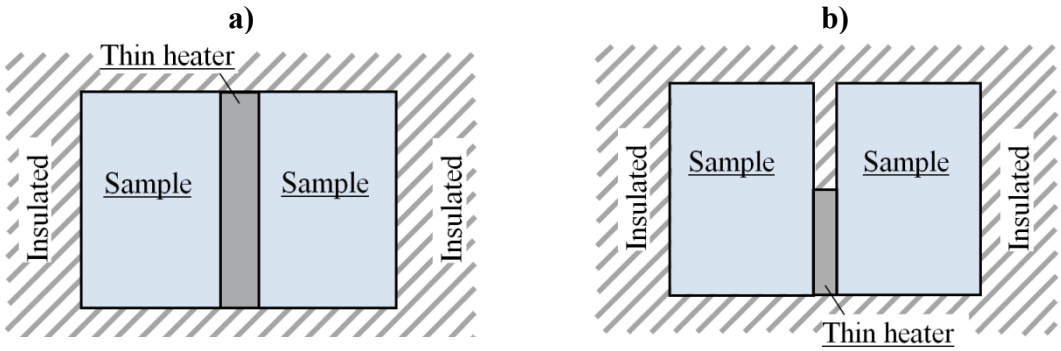

Figure 1. Schematic of the experimental apparatus: uniform heating a), and partial heating b).

Also, in both set-ups the heater dimension along the transversal direction (perpendicular to the plane) is equal to that of the specimens and also all the external surfaces of the device are thermally insulated. Therefore, for the case of figure 1a the heat diffusion can be considered one-dimensional which is suitable only for isotropic materials, while the heat diffusion inside the samples of figure 1b can be treated as two-dimensional instead of three-dimensional. This situation is also preferable for orthotropic materials. Then, for the sake of thermal symmetry, the three-layer configurations (specimen-heater-specimen) shown by figures 1a and 1b reduce to the simplified configurations depicted in figures 2a and 2b, respectively, in which the heater is completely neglected. In particular, figure 2a shows a slab (one of the samples) subject to a uniform surface heat flux at x=0 and insulated at the backside x=L; while figure 2b displays a rectangular domain having all the surfaces insulated except the surface x=0, at which a partial heating is applied from y=0 to y=W_0. Note that as the heat generation occurring inside the heater is assumed uniform, it can be considered as a surface heat flux. Also, in both cases of figure 2 the heat flux is applied for a finite period of time (from t=0 to t_h).

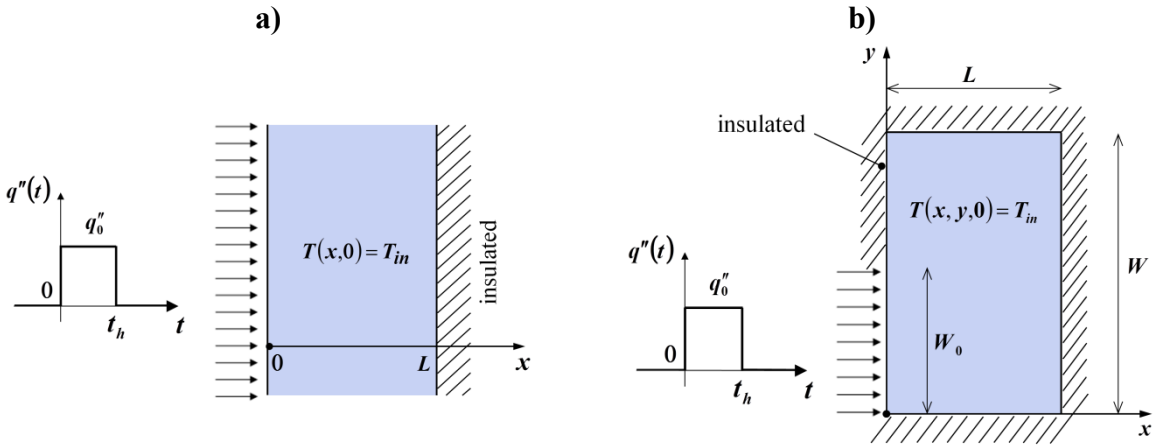

Figure 2. Simplified schematics: one-dimensional finite body for uniform heating a), and two-dimensional domain for piecewise-uniform heating b).

According to the numbering system devised in [26], the two transient heat conduction problems described above may be denoted by X22B50T1 and X22B(y5t5)0Y22B00T1, respectively. In detail, the former denotes a one-dimensional (1D) rectangular finite body (by the "X"), subject to a boundary condition of the second kind at the surface x=0 (by the first "2" in X22) where a finite duration heat flux is applied (by the B5), and having an insulated boundary at x=L (heat flux boundary condition by the last "2" in X22, which is homogeneous by the "0" in B50); also, T1 stands for a uniform initial temperature. The second number denotes a two-dimensional (2D) domain (by the letters X and Y), subject to a partial heating applied at x=0 from t=0 to t=t_h (heat flux boundary condition by the first "2" in "X22" which is discontinuous in both space and time by the "y5t5" in "B(y5t5)0"), and having an insulated boundary at x=L (by the last "2" in "X22" and by the 0 in "B(y5t5)0" for which the heat flux is zero); also "Y22B00" stands for a zero heat flux at both y=0 and y=W, while "T1" has the same meaning of the 1D case.

Note that when in figure 2b $W_0 \to W$ the complex 2D transient problem related to a piecewise-uniform heating reduces to the 1D problem depicted in figure 2a (uniform heating). For this reason in the next section only the 2D problem is stated.

3. Mathematical formulation

The governing equations for the complex 2D problem may be defined as follows

$$\frac{\partial^2 T}{\partial x^2}+\frac{\partial^2 T}{\partial y^2}=\frac{1}{\alpha}\frac{\partial T}{\partial t} \qquad (0<x<L\,,\,0<y<W\,,t>0) \tag{1a}$$

$$-k\left.\frac{\partial T}{\partial x}\right|_{x=0}=q_0''(y,t) \quad (0<y<W\,,t>0) \tag{1b}$$

$$\left.\frac{\partial T}{\partial x}\right|_{x=L}=h_L\left[T(x=L,t)-T_\infty\right] \quad (0<y<W,t>0) \tag{1c}$$

$$\left.\frac{\partial T}{\partial y}\right|_{y=0}=0 \quad (0<x<L,t>0) \tag{1d}$$

$$\left.\frac{\partial T}{\partial y}\right|_{y=W}=0 \quad (0<x<L,t>0) \tag{1e}$$

$$T(x,y,t=0)=T_{in} \quad (0<x<L,0<y<W) \tag{1f}$$

where α is the thermal diffusivity ($\alpha=k^2/\varepsilon^2$) and the surface heat flux $q_0''(y,t)$ is uniform in space but with a step change ($q_0''\to 0$) at $y=W_0$; also, the heat flux is time-dependent as it is constant for $t\le t_h$ while it is zero for $t>t_h$. In mathematical form it results in

$$q_0''(y,t)=\begin{cases} q_0\left[H(t)-H(t-t_h)\right], & \text{for} \quad 0<y<W_0 \\ 0, & \text{for} \quad W_0<y<W \end{cases} \quad (t>0) \tag{2}$$

In the above equation q_0 is the constant heat flux applied for $t\le t_h$, and $H(t)$ denotes the Heaviside unit step function.

Note that in Eq. (1c) the heat transfer coefficient h_L simulates the insulating material in contact with a fluid at temperature T_∞ at $x=L$ (sample backside). In particular, when the sample consists of a high-conductivity material (for instance, a metallic material), it results in $k/L >> h_L$. In such a case, h_L tends to zero and the 3rd kind boundary condition defined by Eq. (1c) reduces to the zero heat flux condition (perfect insulated).

$$\left.\frac{\partial T}{\partial x}\right|_{x=L}=0 \quad (0<y<W,t>0) \tag{3}$$

The validity of equation (3) for metallic materials and short experiment times is always ensured by the small temperatures reached at the sample backside. Notwithstanding, when the experiment times becomes much longer, the mean temperature at the sample backside increases and as a result the heat loss through the insulating material is not negligible. Consequently Eq. (1c) becomes more appropriate and the parameter h_L should be considered in addition to the parameters to be estimated. In such a case a total of three parameters (k, ε and h_L) would be estimated. Alternatively, it is possible to approximate this heat transfer coefficient as $h_L=k_{is}/L_{is}$, that is assuming a known value for it. In other words, modeling like this it would not be a parameter to estimate. In both cases, the model used has to consider the heat transfer coefficient at the sample backside. For such model the temperature solution is available in the specialized literature [27]. However, the aim of the present work is to establish the advantages of using a uniform heating or a piecewise-uniform heating when estimating k and ε, by neglecting the effect of the heat loss. Also, as a matter of fact a metallic sample for not too large experiment times allow the perfect insulated condition to be valid with good approximation. The reader can found a discussion about the effect of the heat loss at the insulated surface on the estimates

of thermal conductivity and volumetric heat capacity obtained through a one-dimensional model in [28].

Using Eq. (3), the 2D transient heat conduction problem is denoted by X22B(y5t5)0Y22B00T1. The temperature solution to this problem is given in dimensionless form in the next Section, where the following dimensionless groups are used

$$\tilde{T}=\frac{T-T_{in}}{q_0''L/k};\quad \tilde{x}=\frac{x}{L};\quad \tilde{y}=\frac{y}{L};\quad \tilde{t}=\frac{k^2t}{\varepsilon^2L^2};\quad \tilde{t}_{\mathrm{h}}=\frac{k^2t_{\mathrm{h}}}{\varepsilon^2L^2};\quad \tilde{W}=\frac{W}{L};\quad \tilde{W}_0=\frac{W_0}{L};\quad \tilde{q}_0''=\frac{q_0''}{q_0}, \tag{4}$$

where $\tilde{x}\in[0,1]$, $\tilde{y}\in\left[0,\tilde{W}\right]$ and $\tilde{t}\geq 0$ is based on the plate length L as well as the heating time $\tilde{t}_h>0$. Note that in dimensionless form the problem notation becomes X22B(y5t5)0Y22B00T0. Also, all the results shown afterwards for the 2D problem are obtained for an aspect ratio $\tilde{W}=2$.

3.1. Temperature solution

The temperature field for the current problem has to be calculated for both $\tilde{t}\leq\tilde{t}_{\mathrm{h}}$ (i.e., during the heating period) and $\tilde{t}_{\mathrm{h}}<\tilde{t}\leq\tilde{t}_{\mathrm{N}}$ (cooling period). By using the superposition principle it may be given as

$$\tilde{T}_{\mathrm{XY22}}^{(\mathrm{B5})}=\begin{cases}\tilde{T}_{\mathrm{XY22}}\left(\tilde{x},\tilde{y},\tilde{t}\right) & \left(0\leq\tilde{t}\leq\tilde{t}_{\mathrm{h}}\right)\\ \tilde{T}_{\mathrm{XY22}}\left(\tilde{x},\tilde{y},\tilde{t}\right)-\tilde{T}_{\mathrm{XY22}}\left(\tilde{x},\tilde{y},\tilde{t}-\tilde{t}_{\mathrm{h}}\right) & \left(\tilde{t}_{\mathrm{h}}<\tilde{t}\leq\tilde{t}_{\mathrm{N}}\right)\end{cases} \tag{5}$$

where $\tilde{t}_N=k^2t_N/\left(\varepsilon^2L^2\right)$ is the dimensionless duration of the experiment, $\tilde{T}_{\mathrm{XY22}}^{(\mathrm{B5})}$ denotes the temperature solution for the addressed problem, and $\tilde{T}_{\mathrm{XY22}}$ stands for the solution to the X22By50Y22B00T0 case in which the partial heating is applied continuously with time. The exact analytical solution for this problem is derived in [25] by means of the Green's Function Solution Equation [29]. In particular, in reference [25] it is determined starting from the product of two Green's functions: one for the x direction and the other one for the y direction. In dimensionless form, it results in

$$\tilde{T}_{\mathrm{XY22}}=-\frac{\tilde{W}_0}{\tilde{W}}\tilde{t}+\frac{\tilde{W}_0}{\tilde{W}}\tilde{T}_{\mathrm{X22}}\left(\tilde{x},\tilde{t}\right)+\tilde{W}^2\tilde{T}_{\mathrm{Y22}}^{(\mathrm{Gy5})}\left(\tilde{y},\tilde{t}\right)+\tilde{T}_{xy}\left(\tilde{x},\tilde{y},\tilde{t}\right) \tag{6a}$$

where

$$\tilde{T}_{\mathrm{X22}}\left(\tilde{x},\tilde{t}\right)=\tilde{t}+\frac{\tilde{x}^2}{2}-\tilde{x}+\frac{1}{3}-2\sum_{m=1}^{\infty}\frac{\cos\left(\beta_m\tilde{x}\right)}{\beta_m^{\,2}}e^{-\beta_m^{\,2}\tilde{t}} \tag{6b}$$

$$\begin{aligned}\tilde{T}_{\mathrm{Y22}}^{(\mathrm{Gy5})}\left(\tilde{y},\tilde{t}\right)=&\frac{\tilde{W}_0}{\tilde{W}^3}\tilde{t}+\frac{1}{12}\left[\tilde{y}_+^3-3\tilde{y}_+^2+2\tilde{y}_+-\tilde{y}_-^3+3\mathrm{sign}\left(\tilde{y}_-\right)\tilde{y}_-^2-2\tilde{y}_-\right]\\&-2\sum_{n=1}^{\infty}\frac{\cos\left(\eta_n\tilde{y}/\tilde{W}\right)\sin\left(\eta_n\tilde{W}_0/\tilde{W}\right)}{\eta_n^{\,3}}e^{-\eta_n^{\,2}\tilde{t}/\tilde{W}^2}\end{aligned} \tag{6c}$$

$$\tilde{T}_{xy}\left(\tilde{x},\tilde{y},\tilde{t}\right)=\left(\frac{1}{3}-\tilde{x}+\frac{\tilde{x}^2}{2}\right)\frac{1-\text{sign}\left(\tilde{y}_-\right)-2\tilde{W}_0/\tilde{W}}{2}$$
$$+\sum_{m=1}^{\infty}\cos\left(\beta_m\tilde{x}\right)\frac{\text{sign}\left(\tilde{y}_-\right)\left(e^{-\beta_m\tilde{W}|\tilde{y}_-|}-e^{-\beta_m\tilde{W}\left(2-|\tilde{y}_-|\right)}-e^{-\beta_m\tilde{W}\tilde{y}_+}+e^{-\beta_m\tilde{W}\left(2-\tilde{y}_+\right)}\right)}{{\beta_m}^2\left(1-e^{-2\beta_m\tilde{W}}\right)} \tag{6d}$$
$$-4\sum_{n=1}^{\infty}\frac{\cos\left(\eta_n\,\tilde{y}/\tilde{W}\right)\sin\left(\eta_n\,\tilde{W}_0/\tilde{W}\right)}{\eta_n}\sum_{m=1}^{\infty}\frac{\cos\left(\beta_m\tilde{x}\right)}{{\beta_m}^2+{\eta_n}^2/\tilde{W}^2}e^{-\left({\beta_m}^2+{\eta_n}^2/\tilde{W}^2\right)\tilde{t}}$$

Also,

$$\tilde{y}_+=\left(\tilde{y}+\tilde{W}_0\right)/\tilde{W};\quad \tilde{y}_-=\left(\tilde{y}-\tilde{W}_0\right)/\tilde{W} \tag{6e}$$

$$\beta_m=m\pi;\quad \eta_n=n\pi \tag{6f}$$

In equation (6f) the symbols β_m and η_n stand for the eigenvalues along the x and y-directions, respectively. Also, the convergence criterion useful to compute the different summations appearing in the above solution are defined in [25].

For the sake of completeness a contour of temperature for the addressed problem at $\tilde{t}$ =1 (with $\tilde{W}$ =2, $\tilde{W}_0$=1 and $\tilde{t}_\text{h}$ =1) is plotted in figure 3.

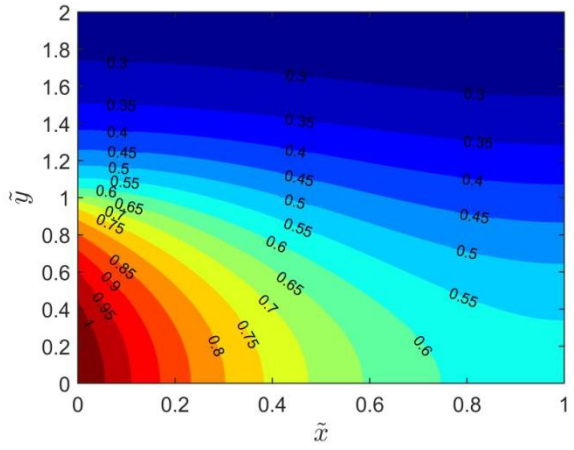

Figure 3. Temperature contour plot for the 2D heat conduction problem.

As mentioned in Section 2, when W_0 goes to W, the complex 2D X22B(x5t5)0Y22B00T0 problem reduces to the 1D X22B50T0 problem, whose exact analytical solution can be still determined by using the superposition principle.

$$\tilde{T}_{\text{X22}}^{(\text{B5})}=\begin{cases}\tilde{T}_{\text{X22}}\left(\tilde{x},\tilde{t}\right) & \left(0\le\tilde{t}\le\tilde{t}_\text{h}\right)\\ \tilde{T}_{\text{X22}}\left(\tilde{x},\tilde{t}\right)-\tilde{T}_{\text{X22}}\left(\tilde{x},\tilde{t}-\tilde{t}_\text{h}\right) & \left(\tilde{t}_\text{h}<\tilde{t}\le\tilde{t}_\text{N}\right)\end{cases} \tag{7}$$

where $\tilde{T}_{\text{X22}}^{(\text{B5})}$ denotes the solution to the X22B50T0 problem, while the solution $\tilde{T}_{\text{X22}}$, related to a slab subject to a uniform surface heat flux at the boundary x=0 and insulated at the other one, is given by Eq. (6b).

4. Parameter estimation and sensitivity coefficients

The sensitivity matrix (i.e. the matrix of the sensitivity coefficients) is involved in the parameter estimation procedure that requires the minimization of the least squares norm. In detail, when using the Gauss method, the following recursive formula is used [30]

$$\underline{b}^{(i+1)} = \underline{b}^{(i)} + \underline{P}^{(i)}\,\underline{Z}^{T(i)}\left[\underline{Y} - \underline{T}^{(i)}\right] \tag{8a}$$

$$\underline{P}^{(i)} = \left[\underline{Z}^{T(i)}\,\underline{Z}^{(i)}\right]^{-1} \tag{8b}$$

where i is the iteration index, $\underline{b}$ stands for the vector of the estimated parameters (in the current case $\underline{b} = [k\ \varepsilon]^T$), $\underline{Y}$ is the measured temperature vector, $\underline{T}$ is the calculated temperature vector and $\underline{Z}$ is the sensitivity matrix. In detail, for the aim of this work the matrix $\underline{Z}$ is defined as follows

$$\underline{Z} = \begin{bmatrix} \underline{Z}(t_1) \\ \underline{Z}(t_2) \\ \vdots \\ \underline{Z}(t_N) \end{bmatrix} \quad \text{with} \quad \underline{Z}(t_j) = \begin{bmatrix} Z_{k,1} & Z_{\varepsilon,1} \\ \vdots & \vdots \\ Z_{k,S} & Z_{\varepsilon,S} \end{bmatrix} \tag{9a}$$

where $Z_{k,s}$ and $Z_{\varepsilon,s}$ (with s=1,2…S) are the sensitivity coefficients of temperature with respect to the parameters k and ε, respectively, computed at the s-th sensor location, at the time t_j (with j=1,…,N). They are

$$Z_{k,s} = \frac{\partial T_s(t_j)}{\partial k}, \qquad Z_{\varepsilon,s} = \frac{\partial T_s(t_j)}{\partial \varepsilon} \tag{9b}$$

To design the optimal experiment, an optimization procedure involving the maximization of the determinant $\left|\underline{Z}^T\underline{Z}\right|$ appearing in Eq. (8b), which is equivalent to the Δ^+ determinant discussed in the next Section, is used. This determinant in fact should be large as possible to ensure the convergence of the iterative procedure defined by equations (8a) and (8b). However, as mentioned in the introduction, the magnitude of the $\left|\underline{Z}^T\underline{Z}\right|$ determinant (or the Δ^+ determinant) also depends on the choice of the parameters to be investigated. In fact, the $\left|\underline{Z}^T\underline{Z}\right|$ determinant related to k and ε is much greater than that obtained when choosing the pair of parameters (k, C) or (k, α); but the proof of this statement it is not the objective of the present work. Moreover, the $\underline{Z}^T\underline{Z}$ matrix not only affects the convergence of the parameters estimation procedure, but also affects the covariance matrix of the estimated parameters (i.e., their uncertainty) as shown in dimensionless form in Subsection 5.1.

4.1. Scaled sensitivity coefficients

Note that the optimization procedure mentioned above does not involve the simple sensitivity coefficients, but it involves the scaled sensitivity coefficients having units of K [31, 32]. In particular, the scaled sensitivity coefficients with respect to the parameters of interest (k and ε) are defined as follows:

$$X_k = kZ_k = k\frac{\partial T}{\partial k}, \qquad X_\varepsilon = \varepsilon Z_\varepsilon = \varepsilon\frac{\partial T}{\partial \varepsilon} \tag{10a}$$

where for the aim of this paper the temperature T may be either the 2D transient solution $T_{\mathrm{XY22}}^{(\mathrm{B5})}$ or the 1D solution $T_{\mathrm{X22}}^{(\mathrm{B5})}$. In dimensionless form they become:

$$\tilde{X}_k = \frac{X_k}{q_0'' L/k}, \qquad \tilde{X}_\varepsilon = \frac{X_\varepsilon}{q_0'' L/k} \tag{10b}$$

In detail, the sensitivity with respect to thermal conductivity k can be expressed as

$$X_k = k\frac{\partial T}{\partial k} = k\frac{\partial}{\partial k}\left(\tilde{T}\frac{q_0'' L}{k}\right) = \frac{q_0'' L}{k}\left(k\frac{\partial \tilde{T}}{\partial k} - \tilde{T}\right) \tag{11}$$

where for the more general 2D heat conduction problem the functional dependence of temperature is

$$\tilde{T} = \tilde{T}_{\mathrm{XY22}}^{(\mathrm{B5})}\left[\tilde{x}, \tilde{y}, \tilde{t}(k,\varepsilon), \tilde{\tau}(k,\varepsilon), \tilde{W}, \tilde{W}_0\right] \tag{12a}$$

Note that in the above equation the variable $\tilde{\tau} = \tilde{t} - \tilde{t}_{\mathrm{h}}$ has been used and it comes from the application of superposition principle, see Eq. (5). Note also that when the simpler 1D problem is considered, Eq. (12a), simplifies as follows

$$\tilde{T} = \tilde{T}_{\mathrm{X22}}^{(\mathrm{B5})}\left[\tilde{x}, \tilde{t}(k,\varepsilon), \tilde{\tau}(k,\varepsilon)\right] \tag{12b}$$

where the variables depending upon the parameters of interest (k and ε) are again $\tilde{t}$ and $\tilde{\tau}$. For this reason the sensitivity coefficients defined afterwards are valid for both 2D and 1D cases.
Therefore, by using the chain rule it is found that

$$\frac{\partial \tilde{T}}{\partial k} = \frac{\partial \tilde{T}}{\partial \tilde{t}}\frac{\partial \tilde{t}}{\partial k} + \frac{\partial \tilde{T}}{\partial \tilde{\tau}}\frac{\partial \tilde{\tau}}{\partial k} \tag{13}$$

The scaled sensitivity coefficient with respect to k is obtained by substituting Eq. (13) in Eq. (11). In dimensionless form it is:

$$\tilde{X}_k = 2\tilde{t}\frac{\partial \tilde{T}}{\partial \tilde{t}} + 2\tilde{\tau}\frac{\partial \tilde{T}}{\partial \tilde{\tau}} - \tilde{T} \tag{14}$$

In the same way, the scaled sensitivity coefficient with respect to thermal effusivity ε is obtained.

$$\tilde{X}_\varepsilon = \varepsilon\frac{\partial \tilde{T}}{\partial \varepsilon} = -2\tilde{t}\frac{\partial \tilde{T}}{\partial \tilde{t}} - 2\tilde{\tau}\frac{\partial \tilde{T}}{\partial \tilde{\tau}} \tag{15}$$

By summing Eq. (14) and (15), the following relationship is obtained

$$\tilde{X}_k + \tilde{X}_\varepsilon = -\tilde{T} \tag{16}$$

4.2. Computation of the scaled sensitivities coefficients

The sensitivity coefficients with respect to k and ε can be computed for both $\tilde{t} \le \tilde{t}_{\mathrm{h}}$ (i.e., during the heating period) and $\tilde{t} > \tilde{t}_{\mathrm{h}}$ (cooling period). By using the superposition principle they may be given as

$$\tilde{X}_{\gamma,\mathrm{XY22}}^{(\mathrm{B5})} = \begin{cases} \tilde{X}_{\gamma,\mathrm{XY22}}\left(\tilde{x}, \tilde{y}, \tilde{t}, \tilde{W}, \tilde{W}_0\right) & \left(0 \le \tilde{t} \le \tilde{t}_{\mathrm{h}}\right) \\ \tilde{X}_{\gamma,\mathrm{XY22}}\left(\tilde{x}, \tilde{y}, \tilde{t}, \tilde{W}, \tilde{W}_0\right) - \tilde{X}_{\gamma,\mathrm{XY22}}\left(\tilde{x}, \tilde{y}, \tilde{\tau}, \tilde{W}, \tilde{W}_0\right) & \left(\tilde{t}_{\mathrm{h}} < \tilde{t} \le \tilde{t}_{\mathrm{N}}\right) \end{cases} \tag{17}$$

where $\gamma = \{k, \varepsilon\}$. Also, bearing in mind Eqs. (14)-(15), the sensitivity coefficients $\tilde{X}_{\gamma,\mathrm{XY22}}\left(\tilde{x},\tilde{y},\tilde{t},\tilde{W},\tilde{W}_0\right)$ related to a continuous heating with time are evaluated using the following relations.

$$\tilde{X}_k\left(\tilde{x},\tilde{y},\tilde{t},\tilde{W},\tilde{W}_0\right) = 2\tilde{t}\,\frac{\partial\tilde{T}}{\partial\tilde{t}} - \tilde{T} \tag{18a}$$

$$\tilde{X}_\varepsilon\left(\tilde{x},\tilde{y},\tilde{t},\tilde{W},\tilde{W}_0\right) = \varepsilon\frac{\partial\tilde{T}}{\partial\varepsilon} = -2\tilde{t}\,\frac{\partial\tilde{T}}{\partial\tilde{t}} \tag{18b}$$

Also, the sensitivities $\tilde{X}_{\gamma,\mathrm{XY22}}\left(\tilde{x},\tilde{y},\tilde{\tau},\tilde{W},\tilde{W}_0\right)$ can be obtained from Eqs. (18a)-(18b) by simply replacing $\tilde{t}$ with $\tilde{\tau} = \tilde{t} - \tilde{t}_\mathrm{h}$. In addition the derivatives appearing in the above sensitivities are computed numerically through a central-difference scheme.

Expressions similar to Eqs. (17), (18a) and (18b) may be used to calculate the sensitivity coefficients for the 1D case. However in such a case the variable $\tilde{y}$ has to be dropped as denoted by Eq. (12b).

Sensitivity coefficients to k and ε evaluated at $\tilde{x} = 0$ are plotted in figure 4 for both cases of uniform and partial heating (for $\tilde{W} = 2$ and $\tilde{W}_0 = 1$). Also, in the latter case different dimensionless locations along the y-direction (i.e., different values of y/L) are considered. By observing figure 4, it is evident that the same sensitivities behave in a quite different way under a uniform (dashed line) or a partial heating (solid lines). Also, in absolute value the greatest sensitivity coefficients are obtained when applying a uniform heating. Note also that, for large times, the sensitivities obtained under a partial heating converge to a unique constant value regardless the y location. Notwithstanding the sensor location along the y-direction affect the optimal experiment discussed afterwards. Furthermore, from a qualitative point of view the sensitivity coefficient to thermal effusivity is less affected by the x-coordinate than the sensitivity to thermal conductivity.

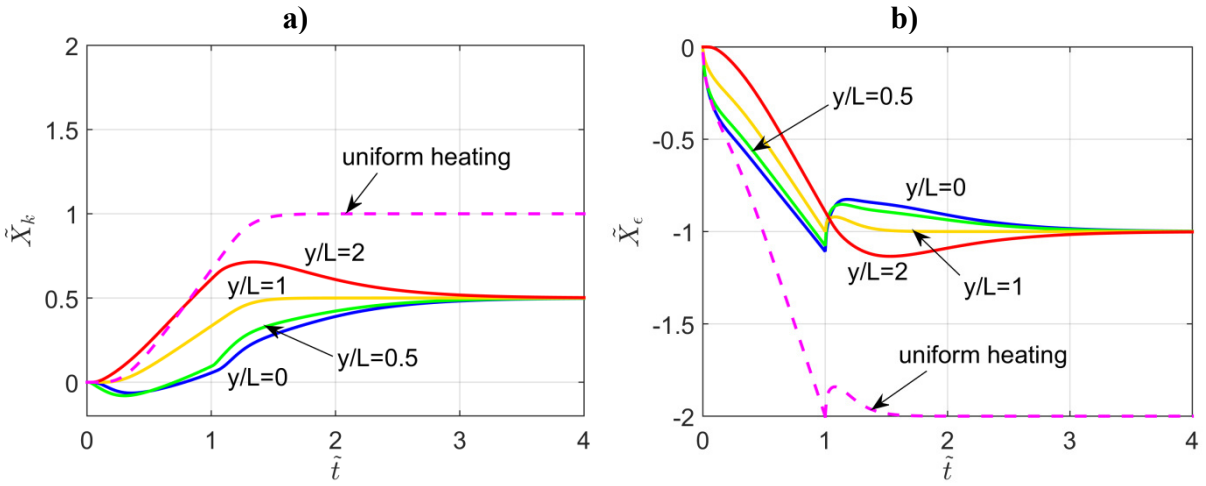

Figure 4. Scaled sensitivity coefficients at $\tilde{x} = 0$ for both uniform (dashed line) and partial heating when $\tilde{W} = 2$ and $\tilde{W}_0 = 1$ (solid lines): a) k and b) ε.

5. Optimal experiment design

The optimal experiment is designed by means of the D-optimum criteria [20, 33] that are based on the maximization of the determinant of the $[\underline{Z}^T \underline{Z}]$ matrix.

In particular, to minimize the confidence region of the estimated parameters (k and ε) the Δ^+ criterion is here used [17, 19 (Chap. 8)]. Specifically, it involves some practical constraints regarding the experiment: 1) a fixed large number of measurements uniformly spaced in time (between $t = 0$ and t_N), and 2) a normalization with respect to the maximum temperature rise reached during the experiment (T_{max} - T_{in}). When k and ε are the parameters to be estimated, this criterion requires the maximization of the following dimensionless determinant

$$\Delta^+ = \begin{vmatrix} \tilde{C}^+_{kk} & \tilde{C}^+_{k\varepsilon} \\ \tilde{C}^+_{\varepsilon k} & \tilde{C}^+_{\varepsilon\varepsilon} \end{vmatrix} = \tilde{C}^+_{kk}\tilde{C}^+_{\varepsilon\varepsilon} - \tilde{C}^{+\,2}_{k\varepsilon} \tag{19a}$$

where $\tilde{C}^+_{\varepsilon k} = \tilde{C}^+_{k\varepsilon}$ has been used. Also, the dimensionless components of Eq. (19a) are defined below

$$\tilde{C}^+_{kk} = \frac{1}{S\tilde{T}^2_{\max}\,\tilde{t}_N} \sum_{s=1}^{S} \int_0^{\tilde{t}_N} \left(\tilde{X}_{s,k}\right)^2 d\tilde{t} \tag{19b}$$

$$\tilde{C}^+_{\varepsilon\varepsilon} = \frac{1}{S\tilde{T}^2_{max}\,\tilde{t}_N} \sum_{s=1}^{S} \int_0^{\tilde{t}_N} \left(\tilde{X}_{s,\varepsilon}\right)^2 d\tilde{t} \tag{19c}$$

$$\tilde{C}^+_{k\varepsilon} = \frac{1}{S\tilde{T}^2_{max}\,\tilde{t}_N} \sum_{s=1}^{S} \int_0^{\tilde{t}_N} \tilde{X}_{s,k}\,\tilde{X}_{s,\varepsilon}\, d\tilde{t} \tag{19d}$$

Also, S stands for the number of temperature sensors used, $\tilde{t}_N$ is the dimensionless duration of the experiment ($\tilde{t}_N = N\,\Delta\tilde{t}$), $\tilde{X}_{s,\gamma}$ (with γ=k, ε) are the dimensionless scaled sensitivity coefficients evaluated at the s-th sensor location, while $\tilde{T}_{\max}$ is the maximum dimensionless temperature reached during the experiment at the corner $\tilde{x} = 0$, $\tilde{y} = 0$.

Note also that, by defining the dimensionless coefficients as shown in Eqs. (19b)-(19d), the determinant Δ^+ is unchanged in value if more than one sensor is placed at the same location.

It is worth noting that the Δ^+ determinant for the 2D problem depends on seven decision variables: the heating and experiment times ($\tilde{t}_h$ and $\tilde{t}_N$), the location of the sensor (x and y coordinates), the number of the sensors (S), the width of the heated region ($\tilde{W}_0$) and the aspect ratio of the sample ($\tilde{W}$), as suggested by the functional dependence of the coefficients defined by Eqs. (19b)-(19d) appearing in Eq. (19a) for the Δ^+. All the variables listed before have been investigated in the design of the optimal experiment with the only exception of the aspect ratio which has been kept constant in the analysis.

5.1. Expected standard deviations

The expected standard deviations related to the optimal experiment aimed at estimating k and ε , simultaneously, can be computed through the covariance matrix of the estimates [19] which in dimensionless form can be taken as

$$\begin{bmatrix} \tilde{\sigma}^2_k & \tilde{\sigma}_{k,\varepsilon} \\ \tilde{\sigma}_{\varepsilon,k} & \tilde{\sigma}^2_\varepsilon \end{bmatrix} = \frac{1}{\Delta^+} \begin{bmatrix} \tilde{C}^+_{\varepsilon\varepsilon} & -\tilde{C}^+_{k\varepsilon} \\ -\tilde{C}^+_{\varepsilon k} & \tilde{C}^+_{kk} \end{bmatrix} \tag{20a}$$

where the determinant Δ^+ and the coefficients $\tilde{C}^+_{kk}$, $\tilde{C}^+_{\varepsilon\varepsilon}$ and $\tilde{C}^+_{\varepsilon k} = \tilde{C}^+_{k\varepsilon}$ are defined by Eqs. (19a)-(19d). Also, the dimensionless standard deviations of k and ε result in

$$\tilde{\sigma}^+_k = \frac{\sigma_k}{k}\frac{(T_{\max} - T_{in})\sqrt{N}}{\sigma} \cong \sqrt{\frac{\tilde{C}^+_{\varepsilon\varepsilon}}{\Delta^+}} \tag{20b}$$

$$\tilde{\sigma}^+_\varepsilon = \frac{\sigma_\varepsilon}{\varepsilon}\frac{(T_{\max} - T_{in})\sqrt{N}}{\sigma} \cong \sqrt{\frac{\tilde{C}^+_{kk}}{\Delta^+}} \tag{20c}$$

Note that in the above equations σ denotes the standard deviation of the measurement error.

6. Results and discussion

In this section the experimental devices sketched in figures 1a (uniform heating) and 1b (partial heating) are compared in terms of their optimal experiments aimed at estimating k and ε. These optimal experiments are designed by maximizing the Δ^+ determinant defined by Eq. (19a) with respect to two experimental variables: 1) the dimensionless duration of the heating $\tilde{t}_h$ and 2) the dimensionless duration of the experiment $\tilde{t}_N$. In detail, this determinant has to be plotted as a function of $\tilde{t}_N$ with $\tilde{t}_h$ as a parameter, as shown for instance by Figure 5 obtained when using a single sensor at ($\tilde{x} = 0$, $\tilde{y} = 0$). This figure highlights that the optimal $\tilde{t}_N$ is the time for which the maximum Δ^+ determinant occurs, while the curve that yields the maximum of the maximum Δ^+ values defines the optimal $\tilde{t}_h$.

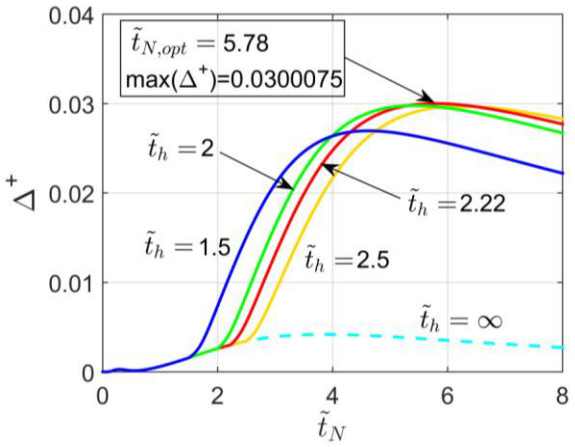

Figure 5. Δ^+ determinant as a function of the experiment duration $\tilde{t}_N$ with the heating duration $\tilde{t}_h$ as a parameter, when using one sensor at the corner ($\tilde{x} = 0$, $\tilde{y} = 0$).

It is worth noting that when a uniform heating is applied to the samples (1D X22B50T0 problem), only two non-embedded sensors locations can be considered, that is, the front-side ($\tilde{x} = 0$) and the back-side ($\tilde{x} = 1$) of the sample; on the contrary when a piecewise-uniform heating is applied, several non-embedded sensors locations are possible along the y direction, as the heat diffusion is two-dimensional. Therefore, for the latter case (X22B(y5t5)0Y22B00T0 problem) the optimal experiment is designed for six different sensors configurations, each of which involves one or more temperature sensors placed in different locations along the y direction. These sensors locations are here denoted as

$\tilde{y}_{1s}$, $\tilde{y}_{2s}$ … where the subscripts "1s", "2s" are referred to the first sensor, or the second one and so on. The six temperature sensors configurations here investigated are discussed afterwards in the following order: a) one sensor (S=1) at $\tilde{x}=0$, b) two sensors (S=2) at $\tilde{x}=0$, c) three sensors (S=3) at $\tilde{x}=0$, d) four sensors (S=4) at $\tilde{x}=0$, e) one sensor at $\tilde{x}=0$ and another at $\tilde{x}=1$, f) two sensors at $\tilde{x}=0$ and other two at $\tilde{x}=1$.

6.1. One sensor at the front side

A comparison between the case of partial heating and that of uniform heating, when using a single temperature sensor at $\tilde{x}=0$, is provided by figure 6. In particular, the Δ^+ determinant and the optimal experiment duration $\tilde{t}_{N,\mathrm{opt}}$ are plotted as a function of the sensor location, with the dimensionless width of the heated region W_0/L as a parameter, in figures 6a and 6b, respectively.

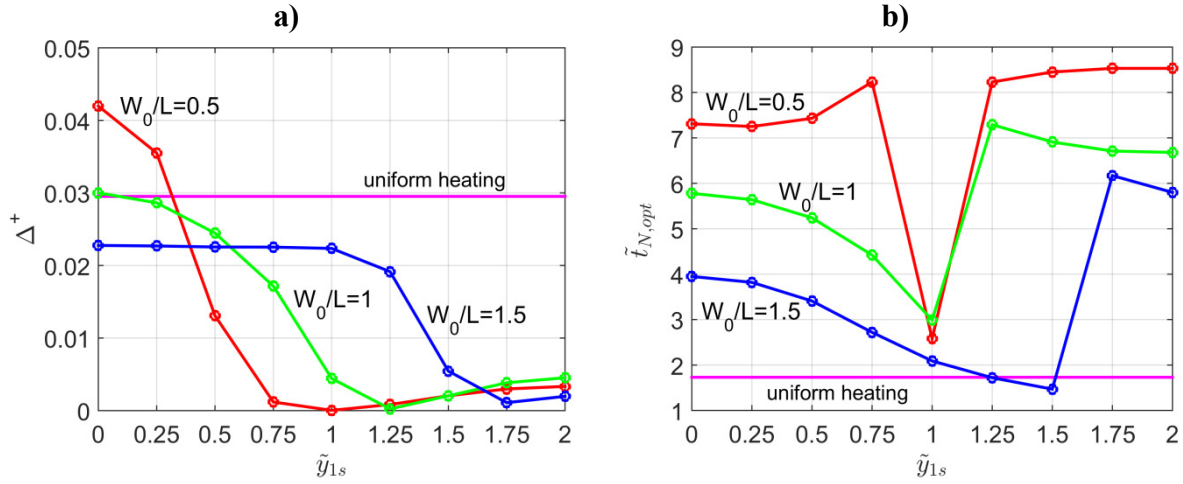

Figure 6. OED when using one sensor at $\tilde{x}=0$: a) Δ^+ determinant and b) optimal experiment duration as a function of the sensor location with W_0/L as a parameter.

From figure 6a one can observe that the partial heating yields small values of the Δ^+ determinant when compared to those obtained when a uniform heating is applied, except for a narrow heated region (W_0/L<1) provide that the temperature sensor is placed near to y=0. However, in such a case a much longer experiment is required as shown by figure 6b. For instance, using a single sensor located at ($\tilde{x}=0, \tilde{y}=0$) for a 2.5 cm-thick stainless steel sample (k=40 W/(mK); ε=380 J/(m^{2}Ks$^{1/2}$)) the optimum experiment should have a duration of about 97 s under a uniform heating, while it should be about four times longer (t_N=411 s) when the same sample is tested using the partially heated set-up. Consequently, the perfect insulated condition at the sample backside is not strictly valid anymore and, therefore, the heat loss through the insulating material has to be considered as discussed in Section 3. On the other hand, the high number of measurements recorded during a longer experiment may yield greater computational efforts in the evaluation of the sensitivity matrix involved in the estimation procedure, see Eqs. (8a)-(8b), as its dimensions increases as shown by Eq. (9a). In fact, for example, using two sensors (i.e., S=2) its dimensions are 1940x2 when performing the shorter experiment (t_N=97 s), while it is a 8220x2 matrix in the longer experiment (t_N=411 s).
Moreover, as shown by figure 6a each Δ^+ curve exhibits a minimum value (close to zero) at a specific sensor location. This is due to high correlation between parameters k and ε occurring at that location and for that particular experimental set-up. Note also that, the minimum value of the Δ^+ determinant is reached with a short experiment duration for a small heated region (W_0/L=0.5), while for wider heated regions it occurs for a longer experiment time (see figure 6b).

6.2. Two sensors at the front side

The results obtained when using two sensors at the surface $\tilde{x} = 0$ for the X22B(y5t5)0Y22B00T0 case are displayed in figures 7 and 8. In detail figure 7 shows the Δ^+ determinant as a function of the second sensor location $\tilde{y}_{2s}$ with the location of the first sensor $\tilde{y}_{1s}$ as a parameter, and for different values of the dimensionless width of the heated region W_0/L; while figure 8 shows the corresponding optimal experiment durations. In both figures a comparison with the optimal experiment obtained when using a uniform heating is also given. It is worth noting that when the locations of the two sensors are equal to each other ($\tilde{y}_{1s} = \tilde{y}_{2s}$), Eqs. (19a)-(19d) yield the same results obtained for a single sensor (marked points with black diamonds in figures 7 and 8).

As shown by figure 7 the highest values of the Δ^+ determinant are obtained when the heating is applied over a small region of the sample front-side (W_0/L=0.5). Note that in such a case when placing the first sensor at $\tilde{y}_{1s} = 0$ or $\tilde{y}_{1s} = 0.25$, the partial heating may yield determinant values higher than that obtained through a uniform heating (see figure 7a). However, figure 8a suggests that in such a case the optimal duration of an experiment performed by applying the partial heating is longer than that required when a uniform heating is applied.

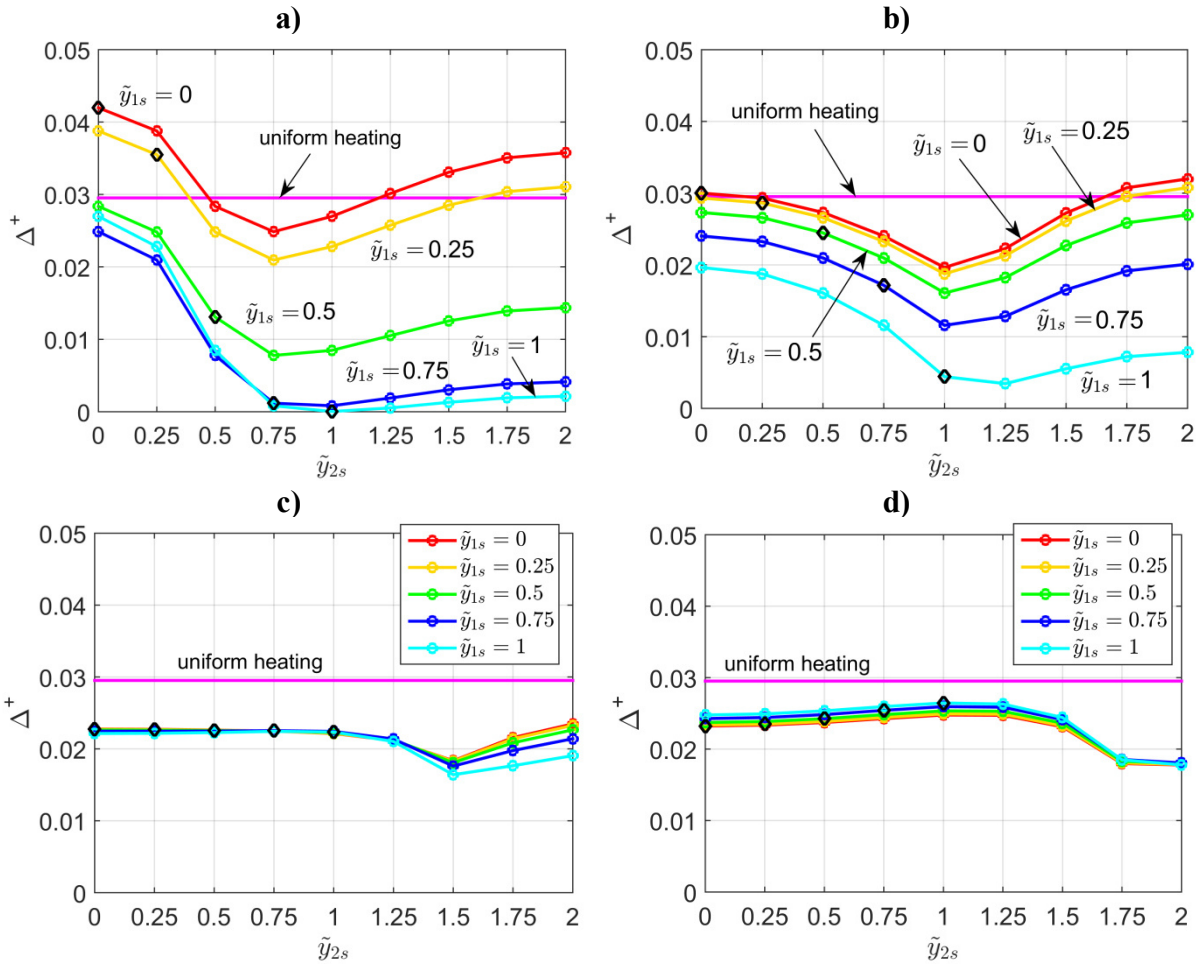

Figure 7. Δ^+ determinant when using two sensors at $\tilde{x} = 0$ for: a) W_0/L=0.5; b) W_0/L=1; c) W_0/L=1.5; d) W_0/L=1.75

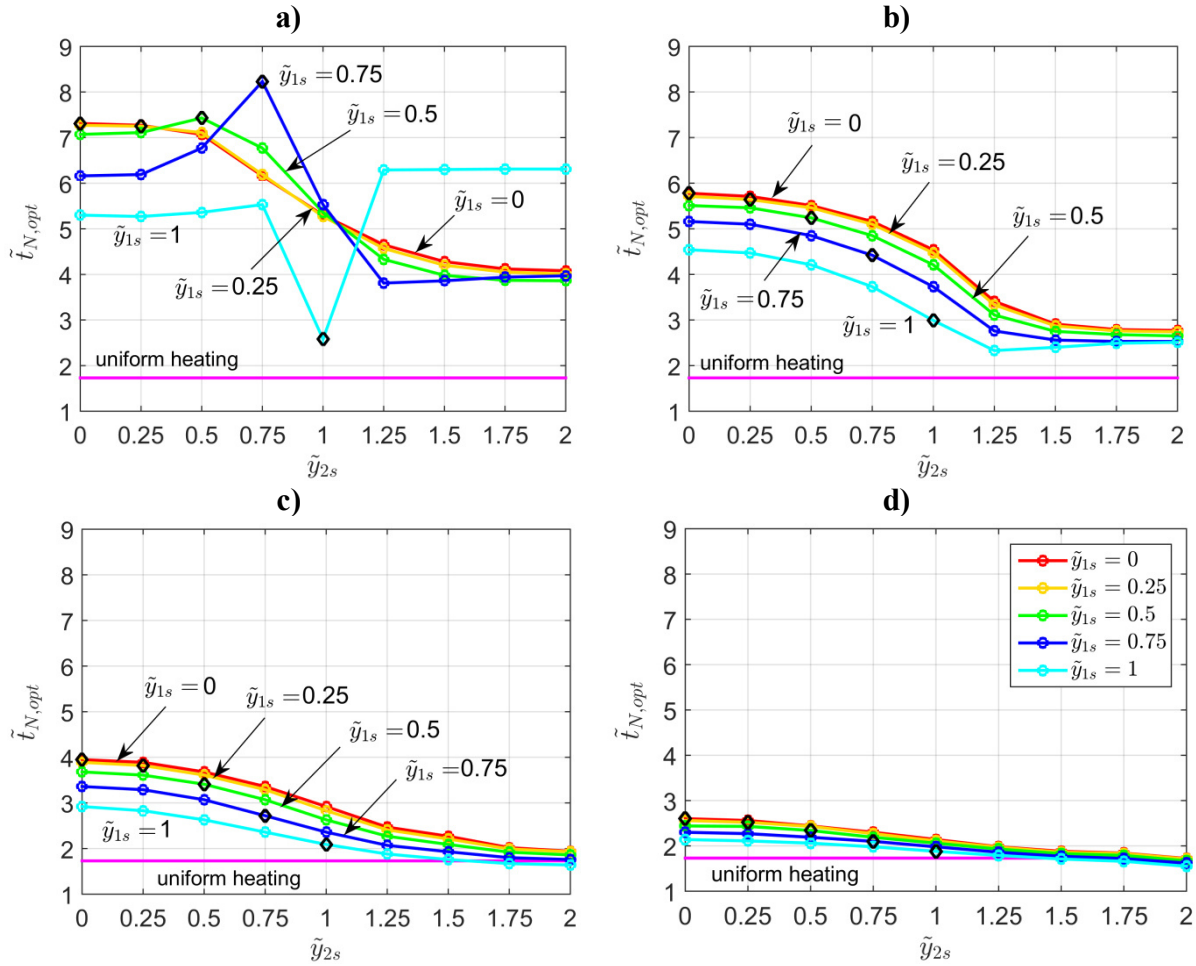

Figure 8. Optimal experiment duration when using two sensors at $\tilde{x}=0$ for:
a) W_0/L=0.5; b) W_0/L=1; c) W_0/L=1.5; d) W_0/L=1.75

6.3. Three sensors at the front side

The case of three temperature sensors placed on the surface $\tilde{x}=0$ has been investigated by considering several combinations of sensors, in which the first of them is placed at $\tilde{y}_{1s}$ =0.25, 0.5 or 0.75. Also, the optimal experiment has been designed for different set-ups of the experimental apparatus i.e., for different values of W_0/L (0.5, 1, 1.5 or 1.75). For the sake of brevity, figure 9 shows only the highest values of the Δ^+ determinant obtained through the best set-ups and the best sensors configurations, together with the related optimal experiment duration. Similarly to the previous figures a comparison with the optimal experiment obtained when applying a uniform heating is also given. As shown by figures 9a, 9c and 9e when using three sensors at the sample front-side, the Δ^+ determinant is lower than or equal to that obtained when using one sensor at $\tilde{x}=0$ under a uniform heating. In particular, the two cases offer the same determinant only when the three sensors are placed at $\tilde{y}_{1s}$ =0.25, $\tilde{y}_{2s}$=0.5, $\tilde{y}_{3s}$=2 , respectively (see figure 9a); however, in such a case the optimal experiment duration is almost doubled compared to the uniform heating case, as shown by figure 9b.

Note that when two of the three sensors are placed in the same location along y (i.e, $\tilde{y}_{1s}=\tilde{y}_{2s}$, $\tilde{y}_{1s}=\tilde{y}_{3s}$ or $\tilde{y}_{2s}=\tilde{y}_{3s}$), the case of three sensors at $\tilde{x}=0$ simply reduces to the case of two sensors discussed in Subsection 6.2 (marked points with black diamonds in figure 9).

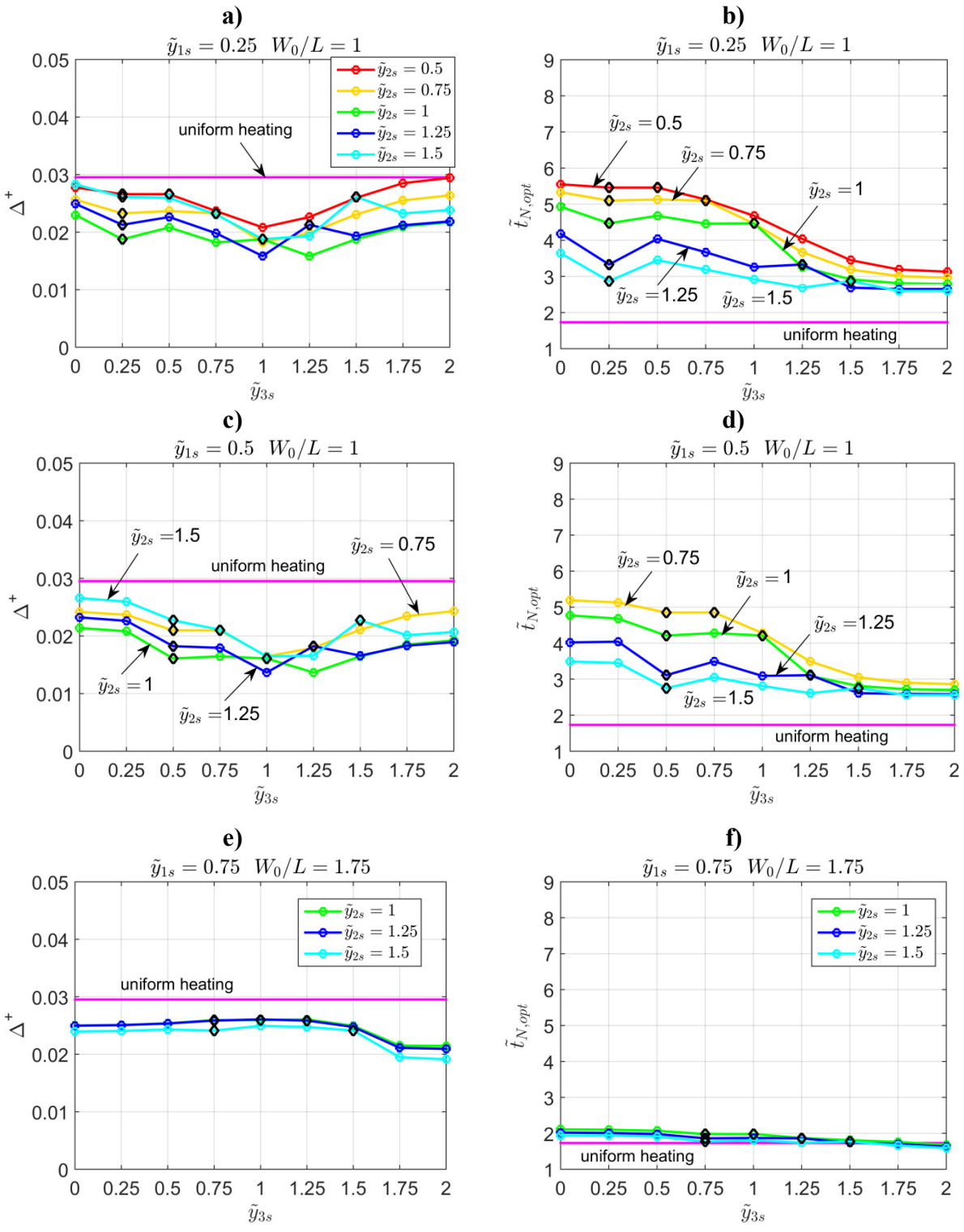

Figure 9. Δ^+ determinant and $\tilde{t}_{N,\mathrm{opt}}$ when using three sensors at $\tilde{x} = 0$ as a function of the third sensor location $\tilde{y}_{3s}$ with the second one location $\tilde{y}_{2s}$ as a parameter and for the best set-up: $\tilde{y}_{1s}$ =0.25 and W_0/L =1 a), b); $\tilde{y}_{1s}$ =0.5 and W_0/L =1 c), d); $\tilde{y}_{1s}$ =0.75 and W_0/L =1.75 e), f).

6.4. Four sensors at the front-side

Due to the large number of possible combinations of four sensors placed at the sample front-side, it is very hard to investigate all of them exhaustively. For this reason table 1 shows the Δ^+ determinant obtained for only some of the most promising combinations (those having at least one or two sensors inside the heated region). Also, the results are given for different values of the dimensionless width of the heated region W_0/L. Moreover, a immediate comparison with the Δ^+ determinant obtained under a uniform heating (using a single sensor at $\tilde{x} = 0$) is provided in the same table. As shown by the table, the maximum values of the determinant obtained for a partial heating (marked in bold) are always lower than the maximum determinant obtained by applying a uniform heating.

Table 1. Δ^+ determinant for different W_0/L when using four temperature sensors.

Sensors locations y/L	max(Δ^+)			uniform heating (X22B50T0)
	W_0/L=0.5	W_0/L =1	W_0/L =1.5	
0.25 0.5 1.25 1.5	0.01963232	0.02213908	0.01986298	
0.25 0.5 1.5 1.75	**0.02166560**	**0.02612014**	0.01972143	
0.25 0.5 1.25 1.75	0.02047604	0.02387740	0.02162392	
0.25 0.75 1.25 1.5	0.01623455	0.01948726	0.01978438	
0.25 0.75 1.5 1.75	0.01795938	0.02315573	0.01935369	
0.25 0.75 1.25 1.75	0.01696826	0.02111908	0.02143736	
0.5 0.75 1.25 1.5	0.00741827	0.01773193	0.01977084	max(Δ^+)
0.5 0.75 1.5 1.75	0.00876020	0.02121005	0.01916393	0.02952076
0.5 0.75 1.25 1.75	0.00800837	0.01929711	0.02135320	
0.25 0.5 0.75 1.25	0.01640470	0.02119326	0.02185144	
0.25 0.5 0.75 1.5	0.01760903	0.02359511	0.02079110	
0.25 0.5 0.75 1.75	0.01846043	0.02543525	0.02277554	
0.25 0.5 0.75 2	0.01876577	0.02611063	**0.02386860**	
0.25 1.25 1.5 1.75	0.01867953	0.01774965	0.01705180	

6.5. One sensor at $\tilde{x} = 0$ and another at $\tilde{x} = 1$

The case of one sensor placed at the sample front side and the other one at the sample backside is now discussed. Several sensor configurations have been tested: in each of them the location of the sensor at $\tilde{x} = 0$ is fixed, while the location of the sensor placed at the sample backside is varied. In particular, five different locations are considered along the y direction that is, y=0, 0.5, 1, 1.5 and 2.

In figures 10a-10c the results obtained using the Δ^+ criterion are plotted as a function of the dimensionless width of the heated region, when the sensor placed at the front side is located at $\tilde{y}_{1s}$ =0, 0.5 and 1, respectively. Note that these are the positions yielding the highest determinant values. In fact, by comparing figures 10a-10c it is evident that to increase the Δ^+ determinant it is needed to locate the front sensor inside the heated region.

Then, from each of these graphs the better sensors collocation has been defined as that that yield the highest Δ^+ determinant, with an optimal experiment duration as brief as possible. The better sensors configurations resulting from this analysis are compared to each other in figure 11, in terms of determinant (figure 11a) and $\tilde{t}_{N,\mathrm{opt}}$ (figure 11b). In both figures 10 and 11 a comparison with the results obtained by applying a uniform heating (using one sensor at $\tilde{x} = 0$ and another one at $\tilde{x} = 1$) is also provided. By observing figure 11a it is possible to state that the partial heating yields Δ^+ determinant values lower than that obtained under a uniform heating. An exception is the case in which the front sensor is placed at $\tilde{y}_{1s}$ =0 and the rear sensor at $\tilde{y}_{1s}$ =2, with a narrow heated region ($\tilde{W}_0 < 0.5$). However, in such a case from one hand the increasing of the Δ^+ determinant is very limited (see figure 11a), but on the other hand the related experiment should be more than four times longer than the optimal one required applying a uniform heating, as shown by figure 11b.

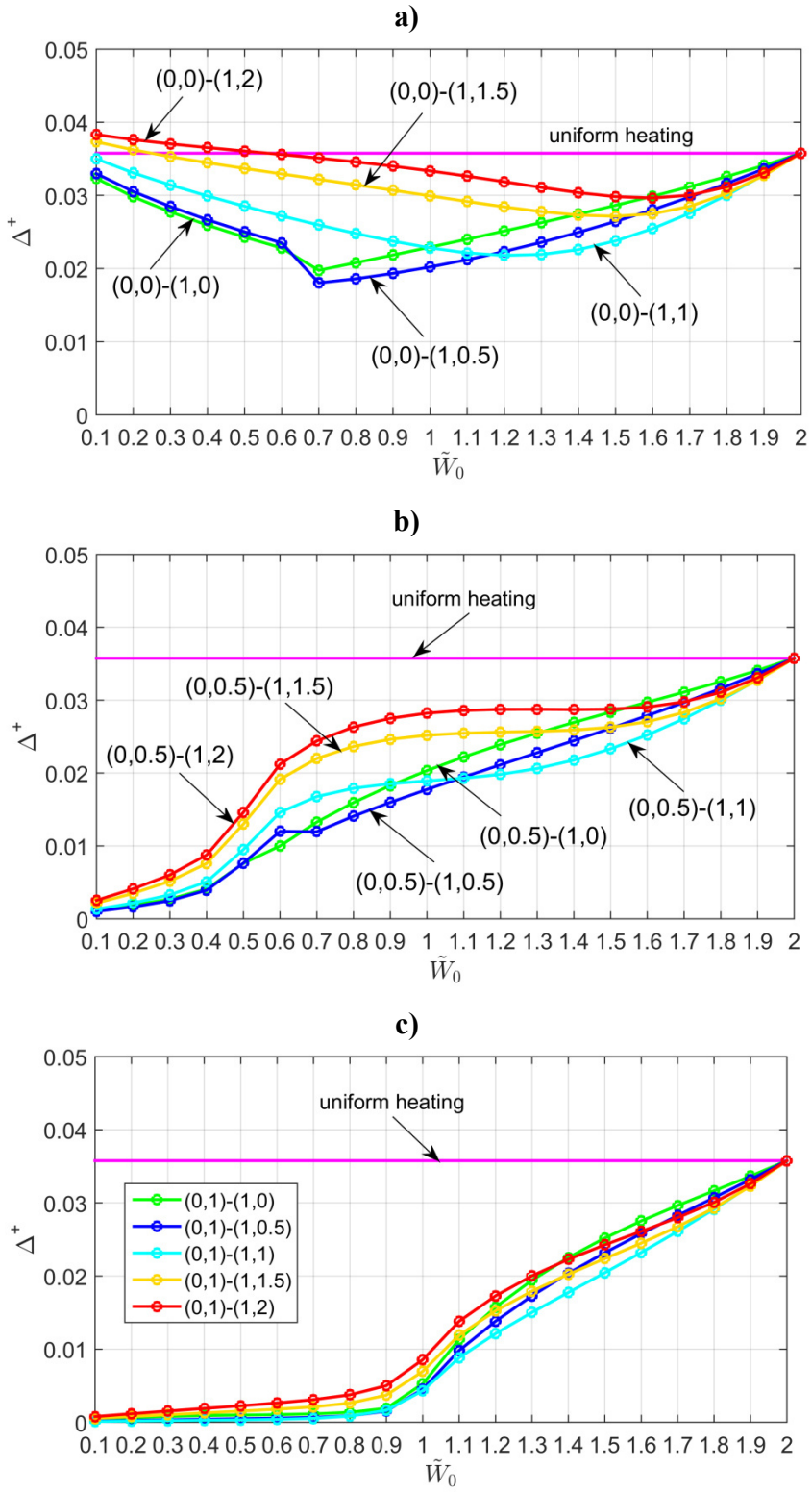

Figure 10. Δ^+ determinant when using two sensors: the former at $\tilde{x} = 0$ located at $\tilde{y}_{1s}$ =0 a), $\tilde{y}_{1s}$ =0.5 b) and $\tilde{y}_{1s}$ =1 c), and the latter placed at $\tilde{x} = 1$ in different positions along the *y*-direction.

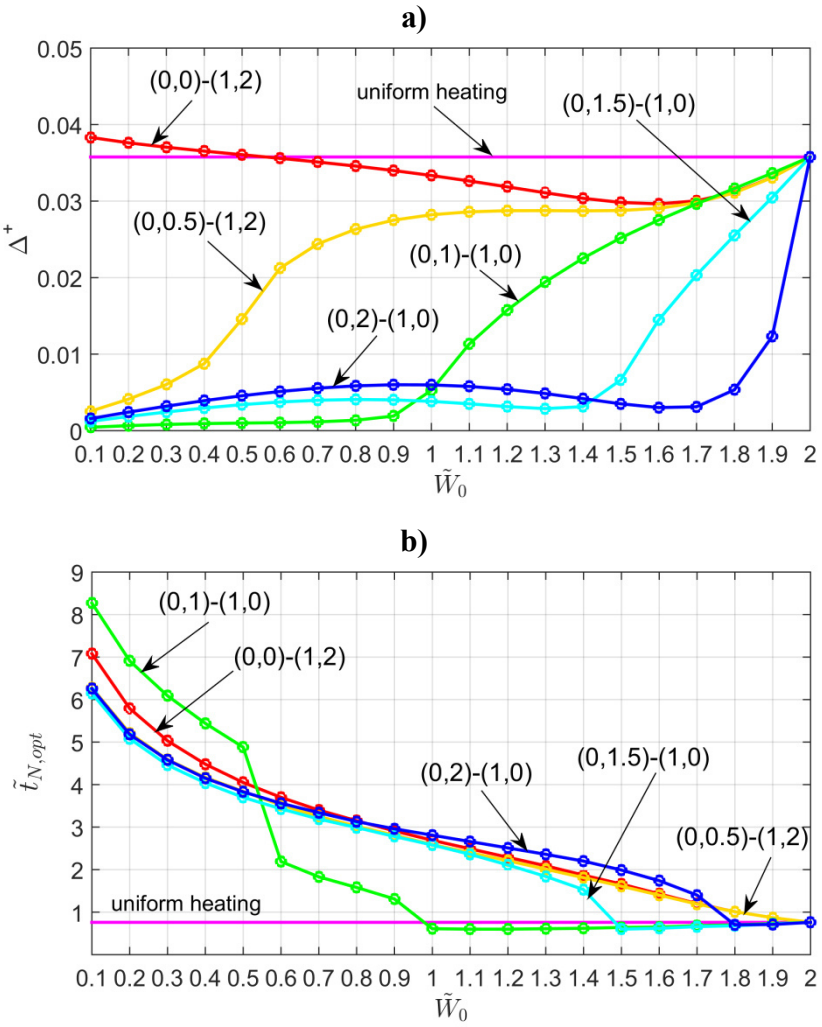

Figure 11. Comparison among the better sensors configurations when using one sensor at the front side and another one at the backside of the sample: a) Δ^+ determinant, and b) optimal experiment duration.

6.6. Two sensors at $\tilde{x}=0$ and two at $\tilde{x}=1$

The last studied case is that involving two sensors at the front side and other two at the sample backside. Due to the large number of possible combinations, the optimization criterion defined by Eqs. (19a)-(19d) has been applied to several configurations having the couple of front sensors (those placed at $\tilde{x}=0$) located in eight different couples of points. For each of these eight couples, the locations of the other two sensors placed at the sample backside have been varied along the *y*-direction.

The results of this analysis have shown that the highest values of the Δ^+ determinant are obtained when the couple of rear sensors are placed at $\tilde{y}=0.75$ and $\tilde{y}=2$. The Δ^+ determinant and the optimal experiment duration related to the five best sensors configurations as a function of the dimensionless width of the heated region, found as described above, are plotted in figures 12a and 12b, respectively. Similarly to the previous cases, a comparison with the results obtained under a uniform heating (using one sensor at $\tilde{x}=0$ and one at $\tilde{x}=1$) is provided in the same figure. As suggested by figure 12, the partial heating yields Δ^+ determinant values lower than that obtained by applying a uniform heating.

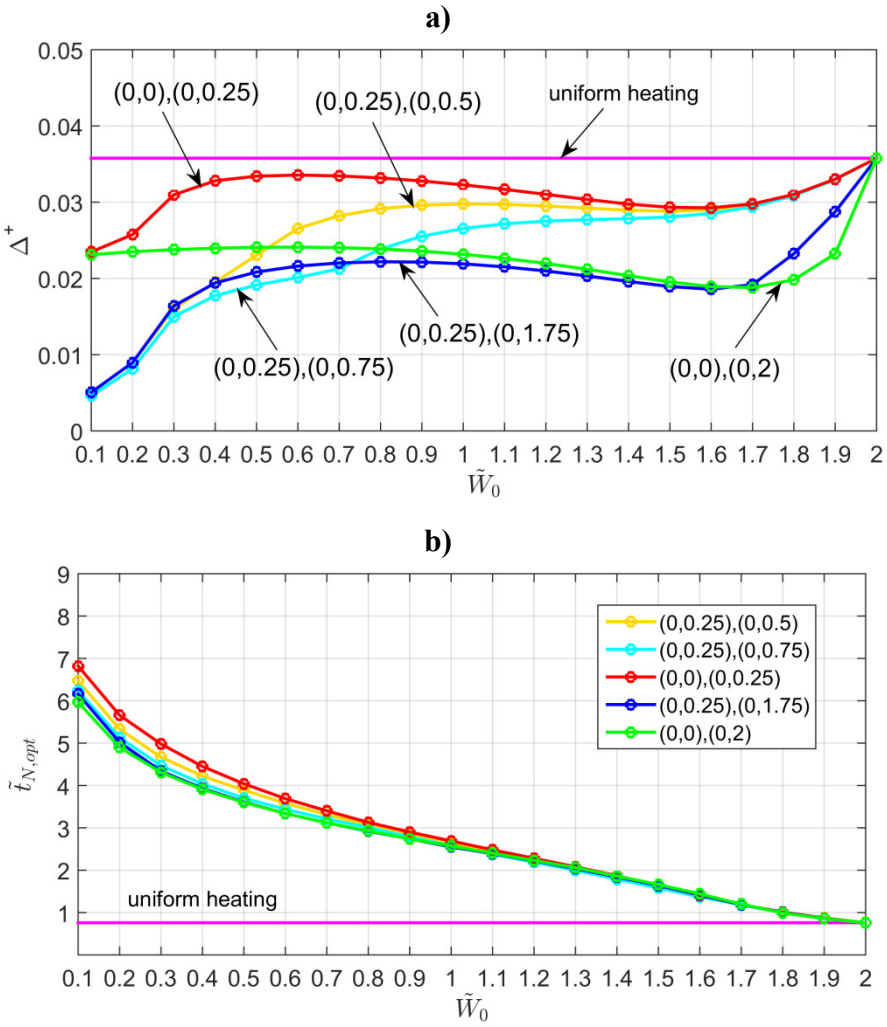

Figure 12. Comparison among the better sensors configurations when using two sensors at the front side and other two located at (1,1.75) and (1,2): a) Δ^+ determinant, and b) optimal experiment duration.

6.7. Expected standard deviations

The expected standard deviations of k and ε when performing the optimal experiment for four sensors configurations are plotted as a function of the dimensionless width of the heated region in figures 13a and 13b, respectively. In detail, the four sensors configurations here considered involve the use of a single sensor at the corner (0,0), a couple of front sensors, one sensor at the front side and another at the sample backside, and four sensors (two at the front side and two at the backside), respectively. For each configuration the optimal experiment designed above, for different values of W_0/L, is used to compute the expected standard deviations through Eqs. (20b) and (20c). Also, a comparison with the standard deviations obtained under a uniform heating using both one sensor at the front side and two sensors (one on the front and one at the rear of the sample) is provided in the same figure.

By observing figure 13 it is evident that the accuracy obtainable for the estimates of k is lower than that expected for the thermal effusivity ε. Although a partial heating may offer a greater accuracy of the estimates of both k and ε especially when using only front sensors, it requires longer experiment times than those required by applying a uniform heating as discussed previously. A small exception is the case of two front sensors located at (0,0) and (0,2) for a dimensionless heated region $1<W_0/L<1.5$.

In fact this experimental set-up would yield a lower $\tilde{\sigma}_k^+$ value and almost the same $\tilde{\sigma}_\varepsilon^+$ obtainable through a uniform heating, but requiring an experiment having approximately the same duration as shown by figures 8b and 8c. However, the corresponding Δ^+ determinant would be less than that obtained under a uniform heating (see figure 7c).

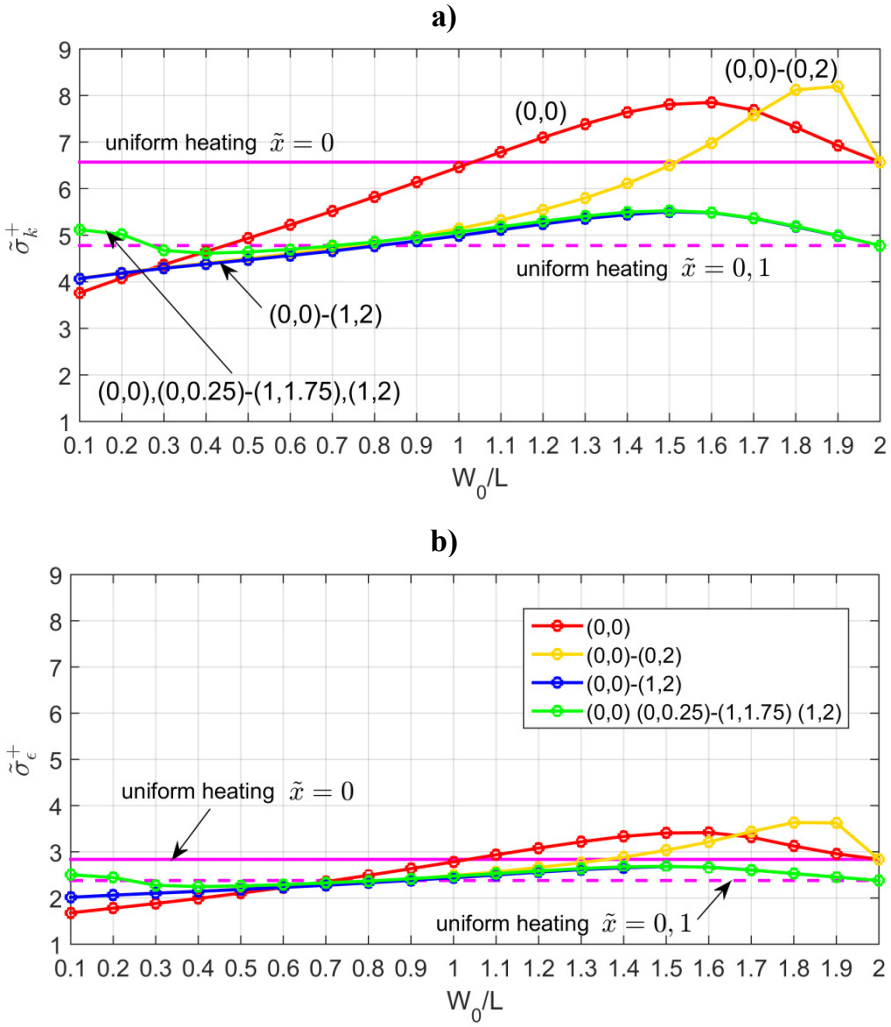

Figure 13. Dimensionless standard deviations related to the optimal experiment for four sensors configurations: a) k, and b) ε.

7. Conclusions

The optimal experiment aimed at estimating k and ε when using the plane source-based experimental apparatus has been designed by applying both a uniform and a piecewise-uniform heating. A D-optimum criterion ensuring a small area of the confidence region of the estimated parameter has been used. The Δ^+ determinant and the related optimal experiment duration obtained for different set-ups and several sensors configurations have been compared in graphical and tabular form. Then the expected standard deviations of k and ε for the best sensors configurations have been also provided. The results of the analysis have shown that the use of a piecewise-uniform heating is not completely beneficial when simultaneously estimating the thermal properties of isotropic materials. In fact, if on

one hand it may offer standard deviations reduced up to about 40% when it is used to estimate k and ε, on the other hand it would require an experiment about four times longer than that required by a uniform heating to ensure a good convergence of the estimation procedure. Therefore, a major computational effort is required.

References

[1] Ahadi M, Andisheh-Tadbir M, Tam M and Bahrami M 2016 An improved transient plane source method for measuring thermal conductivity of thin films: Deconvoluting thermal contact resistance *Int. J. Heat Mass Transfer* **96** 371–380.

[2] Dowding K, Beck J V, Ulbrich A, Blackwell B and Hayes J 1995 Estimation of thermal properties and surface heat flux in carbon-carbon composite *J. Thermophysics Heat Transfer* **9** 2 pp. 345-351.

[3] Hammerschmidt U 2003 A new pulse hot strip sensor for measuring thermal conductivity and thermal diffusivity of solids *Int. J. Thermophysics* **24** 3 pp. 675-682.

[4] Zhang H, Li Y and Tao W 2017 Effect of radiative heat transfer on determining thermal conductivity of semi-transparent materials using transient plane source method *Applied Thermal Eng.* **114** pp. 337-345.

[5] Malheiros F A, Figueiredo A A A, da S. Ignacio L H and Fernandes H C 2019 Estimation of thermal properties using only one surface by means of infrared thermography *Applied Thermal Eng.* **157** 5 113696.

[6] Dowding K J, Beck J V and Blackwell B F 1996 Estimation of directional-dependent thermal properties in a carbon-carbon composite *Int. J. Heat Mass Transf.* **39** 15 3157-3164.

[7] Dowding K J, Blackwell B F and Cochran R J 1998 Application of sensitivity coefficients for heat conduction problems, Sandia Report, Albuquerque, NM, USA, SAND98-0543C.

[8] Aviles-Ramos C and Haji-Sheikh A 2001 Estimation of thermophysical properties of composites using multi-parameter estimation and zeroth-order regularization, *Inverse Prob. Eng.* **9** 507-536.

[9] Mzali F, Sassi L, Jemni A, Ben Nasrallah S and Petit D 2004 Optimal experiment design for the identification of thermo-physical properties of orthotropic solids *Inverse Prob. Sci. Eng.* **12** 193–209.

[10] Rodrigues F A, Orlande H R B and Mejias M M 2004 Use of a single heated surface for the estimation of thermal conductivity components of orthotropic 3D solids *Inverse Prob. Sci. Eng.* **12** 501–517.

[11] de Monte F and Beck J V 2009 Eigen-periodic-in-space surface heating in conduction with application to conductivity measurement of thin films *Int. J. Heat Mass Transf.* **52** 5567–5576.

[12] Malinaric S and Dieska P 2016 Stepwise and pulse transient methods of thermophysical parameters measurement *Int. J. Thermophys.* **37** 12 1–9.

[13] D'Alessandro G and de Monte F 2022 On the optimum experiment and heating times when estimating thermal properties through the plane source method *Heat Transfer Eng.* **43** 257-269.

[14] D'Alessandro G, de Monte F and Amos D E 2019 Effect of heat source and imperfect contact on simultaneous estimation of thermal properties of high conductivity materials *Math. Problems Eng.* **2019** 1–15 Article ID 5945413.

[15] Wouwer A V, Point N, Porteman S and Remy M 2000 An approach to the selection of optimal sensor locations in distributed parameter systems *J Process Control* **10** 291–300.

[16] Berger J, Dutykh D and Mendes N 2017 On the optimal experiment design for heat and moisture parameter estimation *Experimental Thermal and Fluid Science* **81** 109-122.

[17] Taktak R, Beck J V and Scott E P 1993 Optimal experimental design for estimating thermal properties of composite materials *Int. J. Heat Mass Transf.* **36** 12 2977-2986.

[18] D'Alessandro G and de Monte F 2019 Optimal experiment design for thermal property estimation using a boundary condition of the fourth kind with a time limited heating period *Int. J. Heat Mass Transfer* **134** 1268–1282.
[19] Beck J V and Arnold K J 1977 *Parameter Estimation in Engineering and Science* (New York: John Wiley and Sons).
[20] Ucinski D 2005 *Optimal measurement methods for distributed parameter system identification* (CRC Press).
[21] Ruffio E, Saury D and Petit D 2012 Robust experiment design for the estimation of thermophysical parameters using stochastic algorithms *Int. J. Heat Mass Transf.* **55** 2901-2915.
[22] Dieb T M and Tsuda K 2018 *Machine learning-based experimental design in materials science* In *Nanoinformatics*; Tanaka I, Eds.; Springer: Singapore, pp. 65–74.
[23] Wei H, Zhao S, Rong Q and Bao H 2018 Predicting the effective thermal conductivities of composite materials and porous media by machine learning methods *Int. J. Heat Mass Transf.* **127** 908–916.
[24] Gasparin S, Berger J, D'Alessandro G and de Monte F 2022 Optimal experimental design for the assessment of thermophysical properties in existing building walls. In Proceedings of the 10th International Conference on Inverse Problems in Engineering, Francavilla al Mare, Italy, 15-19 May 2022.
[25] Woodbury K A, Najafi H and Beck J V 2017 Exact analytical solution for 2-D transient heat conduction in a rectangle with partial heating on one edge *Int. J. Therm. Sci.* **112** 252-262.
[26] Cole K D, Beck J V, Woodbury A and de Monte F 2014 Intrinsic verification and a heat conduction database *Int. J. Therm. Sci.* **78** 36–47.
[27] McMasters R L, de Monte F and Beck J V 2019 Generalized solution for two-dimensional transient heat conduction problems with partial heating near a corner *ASME J. Heat Transfer* **141** (7) pp. 071301-1 - 071301-8.
[28] Beck J V, Mishra D K and Dolan K D 2017 Utilization of generalized transient heat conduction solutions in parameter estimation in proceedings of the 9th International Conference on Inverse Problems in Engineering ICIPE, Waterloo, Canada, May 23-26 2017.
[29] Cole K D, Beck J V, Haji-Sheikh A and Litkouhi B 2011 *Heat Conduction Using Green's Function 2nd Edition* (Boca Raton FL: CRC Press Taylor&Francis)
[30] McMaster R L, de Monte F and Beck J V 2018 Estimating two heat-conduction parameters from two complementary transient experiments *J. Heat Transfer (ASME)* **140** (7) pp. 071301-1–071301-8.
[31] Blackwell B F, Cochran R J and Dowding K J 1999 Development and implementation of sensitivity coefficient equations for heat conduction problem *Num. Heat Transfer Part B* **36** 15-32.
[32] Mishra D K, Dolan K D, Beck J V and Ozadali F 2017 Use of Scaled Sensitivity Coefficient Relations for Intrinsic Verification of Numerical Codes and Parameter Estimation for Heat Conduction *ASME J. Verification, Validation Uncertainty Quantification* **2** 031005.
[33] Jumabekova A, Berger J, Foucquier A and Dulikravich G S 2020 Searching an optimal experiment observation sequence to estimate the thermal properties of a multilayer wall under real climate conditions *Int. J. Heat Mass Transfer* **155** 119810.

Comparison of uniform and piecewise-uniform heatings when estimating thermal properties of high-conductivity materials

G D'Alessandro[a,*], F de Monte[a], S Gasparin[b], J Berger[c]

[a] Department of Industrial and Information Engineering and Economics, University of L'Aquila, 67100 L'Aquila, Italy
[b] Cerema, BPE Research team, 44200 Nantes, France
[c] Laboratory of Engineering Sciences for the Environment (LaSIE), UMR 7356 CNRS, La Rochelle University, CNRS, 17000, La Rochelle, France

* Correspondig author: giampaolo.dalessandro@univaq.it

Abstract. A D-optimum criterion is applied to the three-layer apparatus used for simultaneously estimating thermal properties (for example, thermal conductivity and effusivity) through the plane source method. The objective is to perform a comparison between uniform heating and piecewise-uniform heating of high-conductivity solid samples. In particular, the latter case is modeled through a two-dimensional heat conduction problem in which a rectangular plate (i.e. the sample) is partially heated at the front boundary through a surface heat flux, while all the other boundaries are kept insulated. The optimal experiment is designed for different set-ups of the experimental apparatus (width of the heated region, number of sensors and their locations). The convergence and the computational efficiency of the estimation iterative procedure are the terms of the comparison, as well as the expected standard deviations of thermal conductivity and effusivity. The results indicate that the use of a piecewise-uniform heating is not completely beneficial for isotropic materials. In fact, if on one hand it may offer standard deviations reduced up to about 40%, on the other hand it would require an experiment about four times longer than that required by a uniform heating to ensure a good convergence of the estimation iterative procedure. Therefore, a major computational effort is required.

Keywords optimal experiment design, D-optimum criterion, uniform and partial heatings, transient heat conduction, thermal properties, uncertainty of the estimates

Nomenclature

$\underline{b}$	estimated parameter vector
C	volumetric heat capacity [J/(m^3°C)]
$\widetilde{C}^{+}_{ij}$	dimensionless coefficient of the $\underline{\widetilde{X}}^{T}\,\underline{\widetilde{X}}$ matrix, with $i, j = k, \varepsilon$
$H(\cdot)$	Heaviside function
h_L	heat transfer coefficient at the sample backside [W/(m^{2}K)]
k	thermal conductivity [W/(mK)]
L	thickness [m]
N	number of measurements

q''	time-dependent heat flux per unit area [W/m^2]
q_0''	uniform surface heat flux per unit area [W/m^2]
S	number of sensors
T	temperature [K]
T_{max}	maximum temperature reached during the experiment [K]
t	time [s]
t_h	heating time [s]
t_N	experiment time [s]
W	width of the rectangular domain [m]
W_0	width of the heated region [m]
X	scaled sensitivity coefficient [K]
$\underline{X}$	scaled sensitivity coefficient matrix [K]
x	space coordinate along the x-direction [m]
y	space coordinate along the y-direction [m]
$\tilde{y}_{i,s}$	dimensionless y-coordinate for the i-th sensor (i=1,2,3)
$\underline{Y}$	simulated temperature matrix [K]
Z	sensitivity coefficient
$\underline{Z}$	sensitivity coefficients matrix

Greek symbols

α	thermal diffusivity [m^2/s]
β_m	m-th dimensionless eigenvalue along the x-direction
γ	generic parameter, with $\gamma = k, \varepsilon$
Δ^+	determinant of the $\underline{\tilde{X}}^T \underline{\tilde{X}}$ matrix
ε	thermal effusivity [J/(m^{2}Ks$^{1/2}$)]
η_n	n-th dimensionless eigenvalue along the y-direction
σ	standard deviation
$\tilde{\sigma}_i^+$	dimensionless standard deviation, with i= k, ε
$\tilde{\tau}$	variable, $\tilde{\tau} = \tilde{t} - \tilde{t}_h$

Subscripts

h	heating
in	initial
m	counting integer for eigenvalues along the x-direction
max	maximum
n	counting integer for eigenvalues along the y-direction
opt	optimal
s	sensor location
$X22$	X22B10T0 case
$Y22$	Y22B00Gy5T0 case
$XY22$	X22By50Y22B00T0 case
xy	transient 2D component of the temperature solution

Superscripts

$(B5)$	temperature solution for finite heating period
~	dimensionless
T	transpose

1. Introduction

Transient methods to estimate the thermal properties of solid materials allow both thermal conductivity and volumetric heat capacity to be measured simultaneously [1-5]. When using these methods different experimental devices can be employed. In particular, some of them involve a nonuniform heating of the sample and are used for estimating the different, directional, thermal conductivities of orthotropic materials. Such nonuniform heating can be applied through both a partial heating [6-10] and a sinusoidal-in-space heating [11]. The former is applied when testing composites and orthotropic materials in general, while the latter is used when thermal properties of thin films are desired. Other experimental apparatuses are based on a uniform heating [2, 12] of the solid specimen which is suitable for the estimation of thermal conductivity, thermal effusivity (or volumetric heat capacity) of isotropic material, such as metals and plastic materials. Note that from an experimental point of view, thermal properties measurement of low conductivity materials requires to approximate an isothermal boundary condition (placing the sample in perfect thermal contact with a high-conductivity material), while an insulated boundary condition is more appropriate when testing metals, as they can be easily insulated having high thermal conductivity.

Among the transient methods, the plane source method [13, 14] for the estimation of thermal properties of high-conductivity solid materials is here of interest. In particular, the three-layer experimental apparatus used in such a case consists of a thin electrical heater sandwiched between two samples of the same material and thickness, having all the boundaries insulated. Depending upon the dimensions of the heater used to heat up the two samples, this apparatus may have two different experimental set-ups. In fact, the use of a heater having the same dimensions of the samples yields a uniform heating of both of them, while when using a smaller one, a piecewise-uniform (partial) heating is supplied. As known the latter set-up is usually used to estimate the directional thermal conductivities of orthotropic materials. However, the aim of the present work is to investigate whether a piecewise-uniform heating may offer some advantages, in terms of convergence and computational efficiency of the parameters estimation procedure, and also accuracy (standard deviations) of the obtained estimates, when estimating simultaneously the thermal properties of isotropic materials as compared to the uniform heating. This comparison is performed by designing the optimal experiment for both set-ups. Specifically, optimal experiment design allows as much of insights and information as possible to be obtained from the recorded temperature data. In fact, in parameter estimation problems it is of great concern that the measured temperatures are sensitive to the unknown parameters of interest in order to obtain reliable and good estimates for them. In other words, optimal experiment design may suggest the optimum sensors locations [10, 15, 16], the optimum heating and experiment times [13, 17, 18], the optimum geometrical sample configuration [9], and the optimum heat flux applied to the sample [9, 16] to obtain the greatest accuracy of the estimated parameters. Also it may provide insight about which quantities can be conveniently estimated. Several optimization criteria have been suggested, such as the D-optimum criteria based on the maximization of the Fisher matrix determinant [19, 20], the E-optimum criteria requiring the maximization of the minimum eigenvalue of the $\underline{X}^T\underline{X}$ matrix [9] and the A-optimum criteria based on the maximization of the trace of the same matrix [21]. Moreover and alternatively, researchers have also tried innovative approaches based on stochastic optimization algorithms [21], machine learning [22, 23] and convex relaxation strategy [24].

A D-optimum criterion, called Δ^+ criterion [19], is here used to design the optimal experiment aimed at estimating simultaneously thermal conductivity k and thermal effusivity ε (with $\varepsilon = \sqrt{kC}$) when using the plane source-based experimental apparatus for the two different set-ups (uniform and partial heating). It is worth to underline that all the results here derived are valid for isotropic materials only. Also, the Δ^+ criterion requires the maximization of the $\underline{\tilde{X}}^T\underline{\tilde{X}}$ determinant (with $\tilde{X}$ the dimensionless scaled sensitivity matrix) whose magnitude not only affects the convergence of the parameters estimation procedure, but also affects the covariance matrix of the estimated parameters and, therefore, their uncertainty. The magnitude of the Δ^+ determinant depends on the choice of the parameters to be estimated. In fact, the choice to estimate k and ε yields a determinant four times

greater than that obtained for the pair k and C. However, for the sake of brevity the proof of that is not discussed here. Moreover, as the optimization procedure stated above involves the sensitivity coefficients of temperature with respect to the properties of interest, the knowledge of the temperature field inside the sample is required for their computation.

For this purpose, the experimental apparatus is modeled by neglecting the thermal inertia of the heater, the surface contact resistance at the sample/heater interface and the heat loss at the sample backside through the insulating material. Note that a complete description of the apparatus including the inertia of the heater and the imperfect contact between heater and sample, when applying a uniform heating, can be found in references [18] and [13,14], respectively.

Therefore, the set-up related to a piecewise-uniform heating is investigated through a two-dimensional heat conduction problem involving a rectangular plate (representing the sample) partially heated at the front boundary through a surface heat flux, and having all its other boundaries insulated. Also, the heater is completely neglected as well as the heat loss at the sample backside. Furthermore, to take into account a finite heating duration, the exact analytical solution is determined by means of the superposition principle starting from a solution available in the literature [25]. After that, the sensitivity coefficients with respect to k and ε are computed through a finite difference scheme. Then, the optimal experiment is designed for different set-ups of the experimental apparatus that is, for different widths of the heated region and for a different number of sensors placed in several non-embedded locations at both the front side and backside of the sample. The Δ^+ determinant and the optimum experiment duration (which are strictly related to the convergence of the estimation procedure and to the computational efficiency of the same procedure, respectively) obtained when the sample is subject to a uniform or a partial heating are compared in both graphical and tabular form. In addition, for the best sensors configurations the related expected standard deviations of k and ε when applying a partial heating are computed and compared with those obtained under a uniform heating.

The paper is organized as follows. Once the problem is described (Section 2), the mathematical model is discussed in Section 3. The sensitivity coefficients are defined in Section 4, while in Section 5 the criterion used to design the optimal experiment and the computation of the standard deviations are treated. Lastly the results are shown and discussed in Section 6.

2. Description of the problem

The experimental apparatus used in the plane source method for thermal properties estimation of high-conductivity solid materials consists of a thin electrical heater sandwiched between two samples of the same material and thickness, which heat up the surface of both samples [13, 14]. In such a way the experimentalist can be sure that the heating power delivered by the heater is equally given to the two samples. Note that the same apparatus may be used to create both a uniform heating, when the heater covers the whole surface of the samples (figure 1a), and a partial heating when the heater covers partially the interface surface between the two samples (figure 1b).

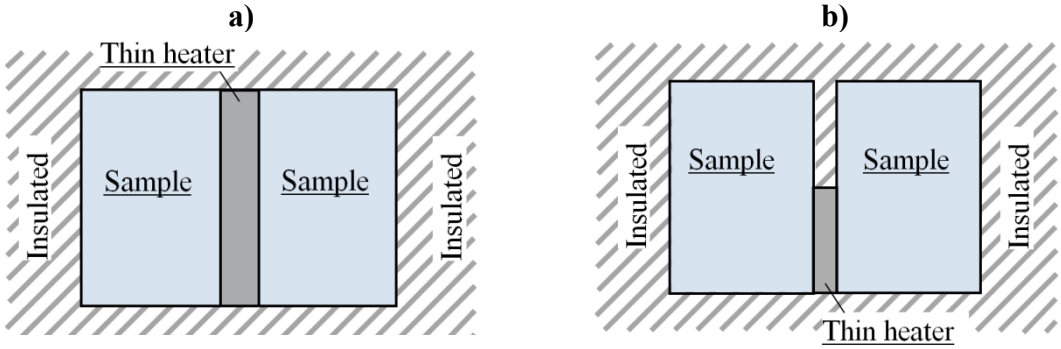

Figure 1. Schematic of the experimental apparatus: uniform heating a), and partial heating b).

Also, in both set-ups the heater dimension along the transversal direction (perpendicular to the plane) is equal to that of the specimens and also all the external surfaces of the device are thermally insulated. Therefore, for the case of figure 1a the heat diffusion can be considered one-dimensional which is suitable only for isotropic materials, while the heat diffusion inside the samples of figure 1b can be treated as two-dimensional instead of three-dimensional. This situation is also preferable for orthotropic materials. Then, for the sake of thermal symmetry, the three-layer configurations (specimen-heater-specimen) shown by figures 1a and 1b reduce to the simplified configurations depicted in figures 2a and 2b, respectively, in which the heater is completely neglected. In particular, figure 2a shows a slab (one of the samples) subject to a uniform surface heat flux at x=0 and insulated at the backside x=L; while figure 2b displays a rectangular domain having all the surfaces insulated except the surface x=0, at which a partial heating is applied from y=0 to y=W_0. Note that as the heat generation occurring inside the heater is assumed uniform, it can be considered as a surface heat flux. Also, in both cases of figure 2 the heat flux is applied for a finite period of time (from t=0 to t_h).

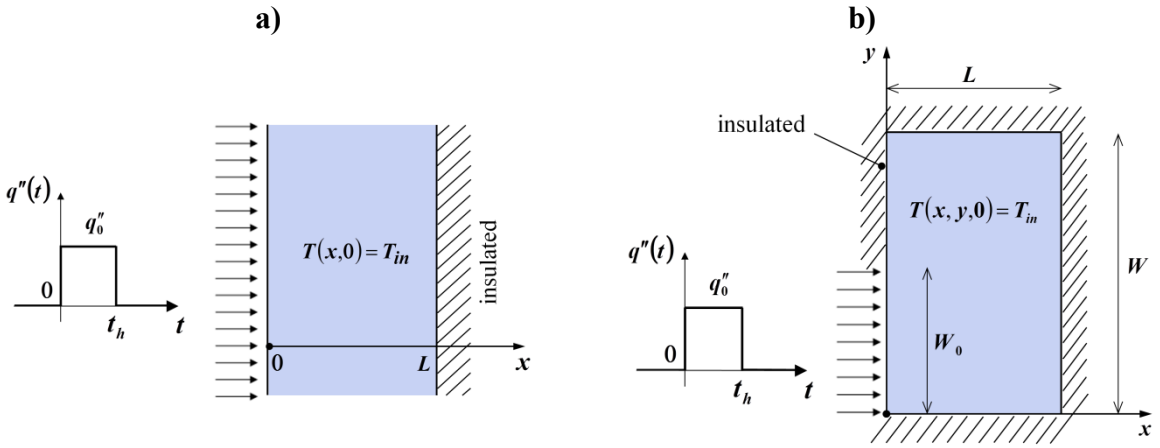

Figure 2. Simplified schematics: one-dimensional finite body for uniform heating a), and two-dimensional domain for piecewise-uniform heating b).

According to the numbering system devised in [26], the two transient heat conduction problems described above may be denoted by X22B50T1 and X22B(y5t5)0Y22B00T1, respectively. In detail, the former denotes a one-dimensional (1D) rectangular finite body (by the "X"), subject to a boundary condition of the second kind at the surface x=0 (by the first "2" in X22) where a finite duration heat flux is applied (by the B5), and having an insulated boundary at x=L (heat flux boundary condition by the last "2" in X22, which is homogeneous by the "0" in B50); also, T1 stands for a uniform initial temperature. The second number denotes a two-dimensional (2D) domain (by the letters X and Y), subject to a partial heating applied at x=0 from t=0 to t=t_h (heat flux boundary condition by the first "2" in "X22" which is discontinuous in both space and time by the "y5t5" in "B(y5t5)0"), and having an insulated boundary at x=L (by the last "2" in "X22" and by the 0 in "B(y5t5)0" for which the heat flux is zero); also "Y22B00" stands for a zero heat flux at both y=0 and y=W, while "T1" has the same meaning of the 1D case.

Note that when in figure 2b $W_0 \to W$ the complex 2D transient problem related to a piecewise-uniform heating reduces to the 1D problem depicted in figure 2a (uniform heating). For this reason in the next section only the 2D problem is stated.

3. Mathematical formulation

The governing equations for the complex 2D problem may be defined as follows

$$\frac{\partial^2 T}{\partial x^2}+\frac{\partial^2 T}{\partial y^2}=\frac{1}{\alpha}\frac{\partial T}{\partial t} \qquad (0<x<L\,,\,0<y<W\,,t>0) \tag{1a}$$

$$-k\left.\frac{\partial T}{\partial x}\right|_{x=0}=q_0''(y,t) \quad (0<y<W\,,t>0) \tag{1b}$$

$$\left.\frac{\partial T}{\partial x}\right|_{x=L}=h_L\left[T(x=L,t)-T_\infty\right] \quad (0<y<W,t>0) \tag{1c}$$

$$\left.\frac{\partial T}{\partial y}\right|_{y=0}=0 \quad (0<x<L,t>0) \tag{1d}$$

$$\left.\frac{\partial T}{\partial y}\right|_{y=W}=0 \quad (0<x<L,t>0) \tag{1e}$$

$$T(x,y,t=0)=T_{in} \quad (0<x<L,0<y<W) \tag{1f}$$

where α is the thermal diffusivity ($\alpha=k^2/\varepsilon^2$) and the surface heat flux $q_0''(y,t)$ is uniform in space but with a step change ($q_0''\to 0$) at $y=W_0$; also, the heat flux is time-dependent as it is constant for $t\le t_h$ while it is zero for $t>t_h$. In mathematical form it results in

$$q_0''(y,t)=\begin{cases} q_0\left[H(t)-H(t-t_h)\right], & \text{for} \quad 0<y<W_0 \\ 0, & \text{for} \quad W_0<y<W \end{cases} \quad (t>0) \tag{2}$$

In the above equation q_0 is the constant heat flux applied for $t\le t_h$, and $H(t)$ denotes the Heaviside unit step function.

Note that in Eq. (1c) the heat transfer coefficient h_L simulates the insulating material in contact with a fluid at temperature T_∞ at $x=L$ (sample backside). In particular, when the sample consists of a high-conductivity material (for instance, a metallic material), it results in $k/L >> h_L$. In such a case, h_L tends to zero and the 3rd kind boundary condition defined by Eq. (1c) reduces to the zero heat flux condition (perfect insulated).

$$\left.\frac{\partial T}{\partial x}\right|_{x=L}=0 \quad (0<y<W,t>0) \tag{3}$$

The validity of equation (3) for metallic materials and short experiment times is always ensured by the small temperatures reached at the sample backside. Notwithstanding, when the experiment times becomes much longer, the mean temperature at the sample backside increases and as a result the heat loss through the insulating material is not negligible. Consequently Eq. (1c) becomes more appropriate and the parameter h_L should be considered in addition to the parameters to be estimated. In such a case a total of three parameters (k, ε and h_L) would be estimated. Alternatively, it is possible to approximate this heat transfer coefficient as $h_L=k_{is}/L_{is}$, that is assuming a known value for it. In other words, modeling like this it would not be a parameter to estimate. In both cases, the model used has to consider the heat transfer coefficient at the sample backside. For such model the temperature solution is available in the specialized literature [27]. However, the aim of the present work is to establish the advantages of using a uniform heating or a piecewise-uniform heating when estimating k and ε, by neglecting the effect of the heat loss. Also, as a matter of fact a metallic sample for not too large experiment times allow the perfect insulated condition to be valid with good approximation. The reader can found a discussion about the effect of the heat loss at the insulated surface on the estimates

of thermal conductivity and volumetric heat capacity obtained through a one-dimensional model in [28].

Using Eq. (3), the 2D transient heat conduction problem is denoted by X22B(y5t5)0Y22B00T1. The temperature solution to this problem is given in dimensionless form in the next Section, where the following dimensionless groups are used

$$\tilde{T}=\frac{T-T_{in}}{q_0''\,L/k};\quad \tilde{x}=\frac{x}{L};\quad \tilde{y}=\frac{y}{L};\quad \tilde{t}=\frac{k^2t}{\varepsilon^2\,L^2};\quad \tilde{t}_{\mathrm{h}}=\frac{k^2t_{\mathrm{h}}}{\varepsilon^2\,L^2};\quad \tilde{W}=\frac{W}{L};\quad \tilde{W}_0=\frac{W_0}{L};\quad \tilde{q}_0''=\frac{q_0''}{q_0},\ (4)$$

where $\tilde{x}\in[0,1]$, $\tilde{y}\in\left[0,\tilde{W}\right]$ and $\tilde{t}\geq 0$ is based on the plate length L as well as the heating time $\tilde{t}_h>0$. Note that in dimensionless form the problem notation becomes X22B(y5t5)0Y22B00T0. Also, all the results shown afterwards for the 2D problem are obtained for an aspect ratio $\tilde{W}=2$.

3.1. Temperature solution

The temperature field for the current problem has to be calculated for both $\tilde{t}\leq\tilde{t}_{\mathrm{h}}$ (i.e., during the heating period) and $\tilde{t}_{\mathrm{h}}<\tilde{t}\leq\tilde{t}_{\mathrm{N}}$ (cooling period). By using the superposition principle it may be given as

$$\tilde{T}_{\mathrm{XY22}}^{(\mathrm{B5})}=\begin{cases}\tilde{T}_{\mathrm{XY22}}\left(\tilde{x},\tilde{y},\tilde{t}\right) & \left(0\leq\tilde{t}\leq\tilde{t}_{\mathrm{h}}\right)\\ \tilde{T}_{\mathrm{XY22}}\left(\tilde{x},\tilde{y},\tilde{t}\right)-\tilde{T}_{\mathrm{XY22}}\left(\tilde{x},\tilde{y},\tilde{t}-\tilde{t}_{\mathrm{h}}\right) & \left(\tilde{t}_{\mathrm{h}}<\tilde{t}\leq\tilde{t}_{\mathrm{N}}\right)\end{cases}\qquad(5)$$

where $\tilde{t}_N=k^2t_N/\left(\varepsilon^2L^2\right)$ is the dimensionless duration of the experiment, $\tilde{T}_{\mathrm{XY22}}^{(\mathrm{B5})}$ denotes the temperature solution for the addressed problem, and $\tilde{T}_{\mathrm{XY22}}$ stands for the solution to the X22By50Y22B00T0 case in which the partial heating is applied continuously with time. The exact analytical solution for this problem is derived in [25] by means of the Green's Function Solution Equation [29]. In particular, in reference [25] it is determined starting from the product of two Green's functions: one for the x direction and the other one for the y direction. In dimensionless form, it results in

$$\tilde{T}_{\mathrm{XY22}}=-\frac{\tilde{W}_0}{\tilde{W}}\tilde{t}+\frac{\tilde{W}_0}{\tilde{W}}\tilde{T}_{\mathrm{X22}}\left(\tilde{x},\tilde{t}\right)+\tilde{W}^{\,2}\tilde{T}_{\mathrm{Y22}}^{(\mathrm{Gy5})}\left(\tilde{y},\tilde{t}\right)+\tilde{T}_{xy}\left(\tilde{x},\tilde{y},\tilde{t}\right)\qquad(6a)$$

where

$$\tilde{T}_{\mathrm{X22}}\left(\tilde{x},\tilde{t}\right)=\tilde{t}+\frac{\tilde{x}^2}{2}-\tilde{x}+\frac{1}{3}-2\sum_{m=1}^{\infty}\frac{\cos\left(\beta_m\tilde{x}\right)}{\beta_m^{\,2}}e^{-\beta_m^{\,2}\tilde{t}}\qquad(6b)$$

$$\begin{aligned}\tilde{T}_{\mathrm{Y22}}^{(\mathrm{Gy5})}\left(\tilde{y},\tilde{t}\right)=&\frac{\tilde{W}_0}{\tilde{W}^3}\tilde{t}+\frac{1}{12}\left[\tilde{y}_+^3-3\tilde{y}_+^2+2\tilde{y}_+-\tilde{y}_-^3+3\,\mathrm{sign}\left(\tilde{y}_-\right)\tilde{y}_-^2-2\tilde{y}_-\right]\\&-2\sum_{n=1}^{\infty}\frac{\cos\left(\eta_n\,\tilde{y}/\tilde{W}\right)\sin\left(\eta_n\tilde{W}_0/\tilde{W}\right)}{\eta_n^{\,3}}e^{-\eta_n^{\,2}\tilde{t}/\tilde{W}^2}\end{aligned}\qquad(6c)$$

$$\tilde{T}_{xy}\left(\tilde{x},\tilde{y},\tilde{t}\right)=\left(\frac{1}{3}-\tilde{x}+\frac{\tilde{x}^2}{2}\right)\frac{1-\operatorname{sign}\left(\tilde{y}_-\right)-2\tilde{W}_0/\tilde{W}}{2}$$
$$+\sum_{m=1}^{\infty}\cos\left(\beta_m\tilde{x}\right)\frac{\operatorname{sign}\left(\tilde{y}_-\right)\left(e^{-\beta_m\tilde{W}|\tilde{y}_-|}-e^{-\beta_m\tilde{W}\left(2-|\tilde{y}_-|\right)}-e^{-\beta_m\tilde{W}\tilde{y}_+}+e^{-\beta_m\tilde{W}\left(2-\tilde{y}_+\right)}\right)}{{\beta_m}^2\left(1-e^{-2\beta_m\tilde{W}}\right)} \tag{6d}$$
$$-4\sum_{n=1}^{\infty}\frac{\cos\left(\eta_n\,\tilde{y}/\tilde{W}\right)\sin\left(\eta_n\,\tilde{W}_0/\tilde{W}\right)}{\eta_n}\sum_{m=1}^{\infty}\frac{\cos\left(\beta_m\tilde{x}\right)}{{\beta_m}^2+{\eta_n}^2/\tilde{W}^2}e^{-\left({\beta_m}^2+{\eta_n}^2/\tilde{W}^2\right)\tilde{t}}$$

Also,

$$\tilde{y}_+=\left(\tilde{y}+\tilde{W}_0\right)/\tilde{W};\quad \tilde{y}_-=\left(\tilde{y}-\tilde{W}_0\right)/\tilde{W} \tag{6e}$$

$$\beta_m=m\pi;\quad \eta_n=n\pi \tag{6f}$$

In equation (6f) the symbols β_m and η_n stand for the eigenvalues along the x and y-directions, respectively. Also, the convergence criterion useful to compute the different summations appearing in the above solution are defined in [25].

For the sake of completeness a contour of temperature for the addressed problem at $\tilde{t}$ =1 (with $\tilde{W}$ =2, $\tilde{W}_0$=1 and $\tilde{t}_{\mathrm{h}}$ =1) is plotted in figure 3.

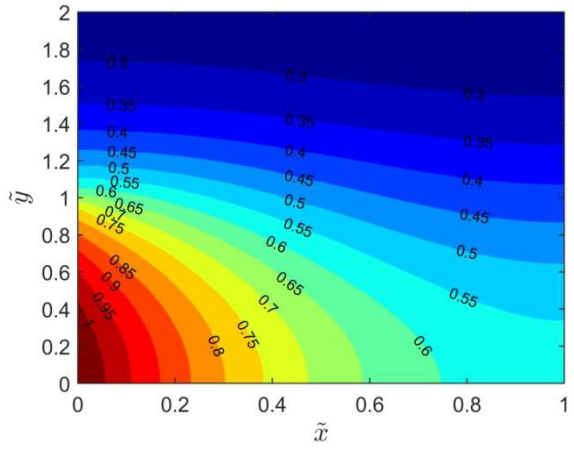

Figure 3. Temperature contour plot for the 2D heat conduction problem.

As mentioned in Section 2, when W_0 goes to W, the complex 2D X22B(x5t5)0Y22B00T0 problem reduces to the 1D X22B50T0 problem, whose exact analytical solution can be still determined by using the superposition principle.

$$\tilde{T}_{\mathrm{X22}}^{(\mathrm{B5})}=\begin{cases}\tilde{T}_{\mathrm{X22}}\left(\tilde{x},\tilde{t}\right) & \left(0\le\tilde{t}\le\tilde{t}_{\mathrm{h}}\right)\\ \tilde{T}_{\mathrm{X22}}\left(\tilde{x},\tilde{t}\right)-\tilde{T}_{\mathrm{X22}}\left(\tilde{x},\tilde{t}-\tilde{t}_{\mathrm{h}}\right) & \left(\tilde{t}_{\mathrm{h}}<\tilde{t}\le\tilde{t}_{\mathrm{N}}\right)\end{cases} \tag{7}$$

where $\tilde{T}_{\mathrm{X22}}^{(\mathrm{B5})}$ denotes the solution to the X22B50T0 problem, while the solution $\tilde{T}_{\mathrm{X22}}$, related to a slab subject to a uniform surface heat flux at the boundary x=0 and insulated at the other one, is given by Eq. (6b).

4. Parameter estimation and sensitivity coefficients

The sensitivity matrix (i.e. the matrix of the sensitivity coefficients) is involved in the parameter estimation procedure that requires the minimization of the least squares norm. In detail, when using the Gauss method, the following recursive formula is used [30]

$$\underline{b}^{(i+1)} = \underline{b}^{(i)} + \underline{P}^{(i)}\,\underline{Z}^{T(i)}\left[\underline{Y} - \underline{T}^{(i)}\right] \tag{8a}$$

$$\underline{P}^{(i)} = \left[\underline{Z}^{T(i)}\,\underline{Z}^{(i)}\right]^{-1} \tag{8b}$$

where i is the iteration index, $\underline{b}$ stands for the vector of the estimated parameters (in the current case $\underline{b} = [k\ \varepsilon]^T$), $\underline{Y}$ is the measured temperature vector, $\underline{T}$ is the calculated temperature vector and $\underline{Z}$ is the sensitivity matrix. In detail, for the aim of this work the matrix $\underline{Z}$ is defined as follows

$$\underline{Z} = \begin{bmatrix} \underline{Z}(t_1) \\ \underline{Z}(t_2) \\ \vdots \\ \underline{Z}(t_N) \end{bmatrix} \quad \text{with} \quad \underline{Z}(t_j) = \begin{bmatrix} Z_{k,1} & Z_{\varepsilon,1} \\ \vdots & \vdots \\ Z_{k,S} & Z_{\varepsilon,S} \end{bmatrix} \tag{9a}$$

where $Z_{k,s}$ and $Z_{\varepsilon,s}$ (with s=1,2…S) are the sensitivity coefficients of temperature with respect to the parameters k and ε, respectively, computed at the s-th sensor location, at the time t_j (with j=1,…,N). They are

$$Z_{k,s} = \frac{\partial T_s(t_j)}{\partial k}, \qquad Z_{\varepsilon,s} = \frac{\partial T_s(t_j)}{\partial \varepsilon} \tag{9b}$$

To design the optimal experiment, an optimization procedure involving the maximization of the determinant $\left|\underline{Z}^T\underline{Z}\right|$ appearing in Eq. (8b), which is equivalent to the Δ^+ determinant discussed in the next Section, is used. This determinant in fact should be large as possible to ensure the convergence of the iterative procedure defined by equations (8a) and (8b). However, as mentioned in the introduction, the magnitude of the $\left|\underline{Z}^T\underline{Z}\right|$ determinant (or the Δ^+ determinant) also depends on the choice of the parameters to be investigated. In fact, the $\left|\underline{Z}^T\underline{Z}\right|$ determinant related to k and ε is much greater than that obtained when choosing the pair of parameters (k, C) or (k, α); but the proof of this statement it is not the objective of the present work. Moreover, the $\underline{Z}^T\underline{Z}$ matrix not only affects the convergence of the parameters estimation procedure, but also affects the covariance matrix of the estimated parameters (i.e., their uncertainty) as shown in dimensionless form in Subsection 5.1.

4.1. Scaled sensitivity coefficients

Note that the optimization procedure mentioned above does not involve the simple sensitivity coefficients, but it involves the scaled sensitivity coefficients having units of K [31, 32]. In particular, the scaled sensitivity coefficients with respect to the parameters of interest (k and ε) are defined as follows:

$$X_k = kZ_k = k\frac{\partial T}{\partial k}, \qquad X_\varepsilon = \varepsilon Z_\varepsilon = \varepsilon\frac{\partial T}{\partial \varepsilon} \tag{10a}$$

where for the aim of this paper the temperature T may be either the 2D transient solution $T_{\mathrm{XY22}}^{(\mathrm{B5})}$ or the 1D solution $T_{\mathrm{X22}}^{(\mathrm{B5})}$. In dimensionless form they become:

$$\tilde{X}_k = \frac{X_k}{q_0'' L / k}, \qquad \tilde{X}_\varepsilon = \frac{X_\varepsilon}{q_0'' L / k} \tag{10b}$$

In detail, the sensitivity with respect to thermal conductivity k can be expressed as

$$X_k = k \frac{\partial T}{\partial k} = k \frac{\partial}{\partial k}\left(\tilde{T} \frac{q_0'' L}{k} \right) = \frac{q_0'' L}{k}\left(k \frac{\partial \tilde{T}}{\partial k} - \tilde{T} \right) \tag{11}$$

where for the more general 2D heat conduction problem the functional dependence of temperature is

$$\tilde{T} = \tilde{T}_{\mathrm{XY22}}^{(\mathrm{B5})}\left[\tilde{x}, \tilde{y}, \tilde{t}(k,\varepsilon), \tilde{\tau}(k,\varepsilon), \tilde{W}, \tilde{W}_0 \right] \tag{12a}$$

Note that in the above equation the variable $\tilde{\tau} = \tilde{t} - \tilde{t}_{\mathrm{h}}$ has been used and it comes from the application of superposition principle, see Eq. (5). Note also that when the simpler 1D problem is considered, Eq. (12a), simplifies as follows

$$\tilde{T} = \tilde{T}_{\mathrm{X22}}^{(\mathrm{B5})}\left[\tilde{x}, \tilde{t}(k,\varepsilon), \tilde{\tau}(k,\varepsilon) \right] \tag{12b}$$

where the variables depending upon the parameters of interest (k and ε) are again $\tilde{t}$ and $\tilde{\tau}$. For this reason the sensitivity coefficients defined afterwards are valid for both 2D and 1D cases.
Therefore, by using the chain rule it is found that

$$\frac{\partial \tilde{T}}{\partial k} = \frac{\partial \tilde{T}}{\partial \tilde{t}} \frac{\partial \tilde{t}}{\partial k} + \frac{\partial \tilde{T}}{\partial \tilde{\tau}} \frac{\partial \tilde{\tau}}{\partial k} \tag{13}$$

The scaled sensitivity coefficient with respect to k is obtained by substituting Eq. (13) in Eq. (11). In dimensionless form it is:

$$\tilde{X}_k = 2\tilde{t} \frac{\partial \tilde{T}}{\partial \tilde{t}} + 2\tilde{\tau} \frac{\partial \tilde{T}}{\partial \tilde{\tau}} - \tilde{T} \tag{14}$$

In the same way, the scaled sensitivity coefficient with respect to thermal effusivity ε is obtained.

$$\tilde{X}_\varepsilon = \varepsilon \frac{\partial \tilde{T}}{\partial \varepsilon} = -2\tilde{t} \frac{\partial \tilde{T}}{\partial \tilde{t}} - 2\tilde{\tau} \frac{\partial \tilde{T}}{\partial \tilde{\tau}} \tag{15}$$

By summing Eq. (14) and (15), the following relationship is obtained

$$\tilde{X}_k + \tilde{X}_\varepsilon = -\tilde{T} \tag{16}$$

4.2. Computation of the scaled sensitivities coefficients

The sensitivity coefficients with respect to k and ε can be computed for both $\tilde{t} \le \tilde{t}_{\mathrm{h}}$ (i.e., during the heating period) and $\tilde{t} > \tilde{t}_{\mathrm{h}}$ (cooling period). By using the superposition principle they may be given as

$$\tilde{X}_{\gamma,\mathrm{XY22}}^{(\mathrm{B5})} = \begin{cases} \tilde{X}_{\gamma,\mathrm{XY22}}\left(\tilde{x}, \tilde{y}, \tilde{t}, \tilde{W}, \tilde{W}_0 \right) & \left(0 \le \tilde{t} \le \tilde{t}_{\mathrm{h}} \right) \\ \tilde{X}_{\gamma,\mathrm{XY22}}\left(\tilde{x}, \tilde{y}, \tilde{t}, \tilde{W}, \tilde{W}_0 \right) - \tilde{X}_{\gamma,\mathrm{XY22}}\left(\tilde{x}, \tilde{y}, \tilde{\tau}, \tilde{W}, \tilde{W}_0 \right) & \left(\tilde{t}_{\mathrm{h}} < \tilde{t} \le \tilde{t}_{\mathrm{N}} \right) \end{cases} \tag{17}$$

where $\gamma = \{k, \varepsilon\}$. Also, bearing in mind Eqs. (14)-(15), the sensitivity coefficients $\tilde{X}_{\gamma,\mathrm{XY22}}\left(\tilde{x},\tilde{y},\tilde{t},\tilde{W},\tilde{W}_0\right)$ related to a continuous heating with time are evaluated using the following relations.

$$\tilde{X}_k\left(\tilde{x},\tilde{y},\tilde{t},\tilde{W},\tilde{W}_0\right) = 2\tilde{t}\,\frac{\partial \tilde{T}}{\partial \tilde{t}} - \tilde{T} \tag{18a}$$

$$\tilde{X}_\varepsilon\left(\tilde{x},\tilde{y},\tilde{t},\tilde{W},\tilde{W}_0\right) = \varepsilon\frac{\partial \tilde{T}}{\partial \varepsilon} = -2\tilde{t}\,\frac{\partial \tilde{T}}{\partial \tilde{t}} \tag{18b}$$

Also, the sensitivities $\tilde{X}_{\gamma,\mathrm{XY22}}\left(\tilde{x},\tilde{y},\tilde{\tau},\tilde{W},\tilde{W}_0\right)$ can be obtained from Eqs. (18a)-(18b) by simply replacing $\tilde{t}$ with $\tilde{\tau} = \tilde{t} - \tilde{t}_\mathrm{h}$. In addition the derivatives appearing in the above sensitivities are computed numerically through a central-difference scheme.

Expressions similar to Eqs. (17), (18a) and (18b) may be used to calculate the sensitivity coefficients for the 1D case. However in such a case the variable $\tilde{y}$ has to be dropped as denoted by Eq. (12b).

Sensitivity coefficients to k and ε evaluated at $\tilde{x} = 0$ are plotted in figure 4 for both cases of uniform and partial heating (for $\tilde{W} = 2$ and $\tilde{W}_0 = 1$). Also, in the latter case different dimensionless locations along the y-direction (i.e., different values of y/L) are considered. By observing figure 4, it is evident that the same sensitivities behave in a quite different way under a uniform (dashed line) or a partial heating (solid lines). Also, in absolute value the greatest sensitivity coefficients are obtained when applying a uniform heating. Note also that, for large times, the sensitivities obtained under a partial heating converge to a unique constant value regardless the y location. Notwithstanding the sensor location along the y-direction affect the optimal experiment discussed afterwards. Furthermore, from a qualitative point of view the sensitivity coefficient to thermal effusivity is less affected by the x-coordinate than the sensitivity to thermal conductivity.

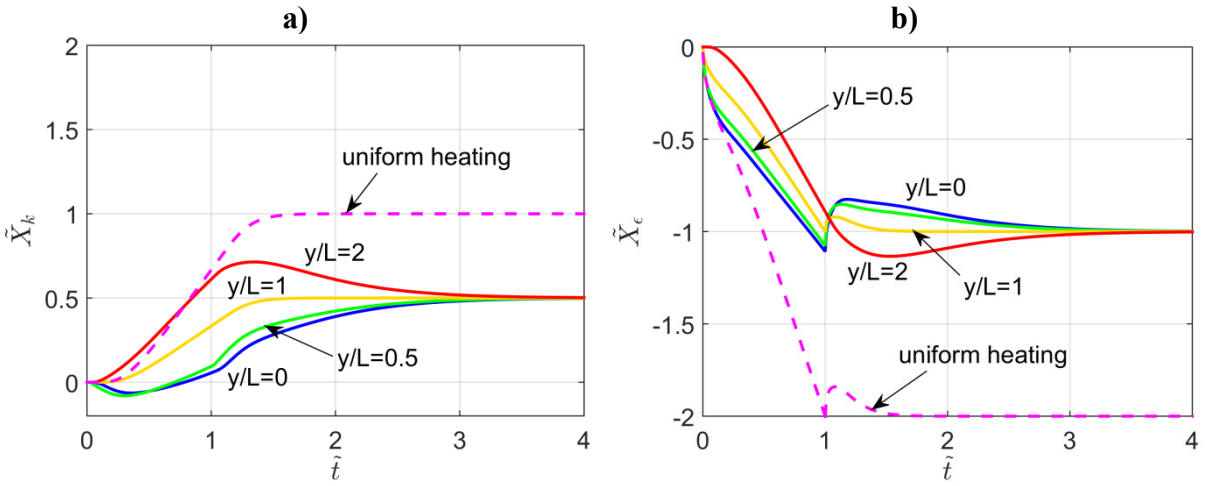

Figure 4. Scaled sensitivity coefficients at $\tilde{x} = 0$ for both uniform (dashed line) and partial heating when $\tilde{W} = 2$ and $\tilde{W}_0 = 1$ (solid lines): a) k and b) ε.

5. Optimal experiment design

The optimal experiment is designed by means of the D-optimum criteria [20, 33] that are based on the maximization of the determinant of the $[\underline{Z}^T \underline{Z}]$ matrix.

In particular, to minimize the confidence region of the estimated parameters (k and ε) the Δ^+ criterion is here used [17, 19 (Chap. 8)]. Specifically, it involves some practical constraints regarding the experiment: 1) a fixed large number of measurements uniformly spaced in time (between $t = 0$ and t_N), and 2) a normalization with respect to the maximum temperature rise reached during the experiment (T_{max} - T_{in}). When k and ε are the parameters to be estimated, this criterion requires the maximization of the following dimensionless determinant

$$\Delta^+ = \begin{vmatrix} \tilde{C}^+_{kk} & \tilde{C}^+_{k\varepsilon} \\ \tilde{C}^+_{\varepsilon k} & \tilde{C}^+_{\varepsilon\varepsilon} \end{vmatrix} = \tilde{C}^+_{kk}\tilde{C}^+_{\varepsilon\varepsilon} - \tilde{C}^{+\,2}_{k\varepsilon} \tag{19a}$$

where $\tilde{C}^+_{\varepsilon k} = \tilde{C}^+_{k\varepsilon}$ has been used. Also, the dimensionless components of Eq. (19a) are defined below

$$\tilde{C}^+_{kk} = \frac{1}{S\tilde{T}^2_{\max}\,\tilde{t}_N} \sum_{s=1}^{S} \int_0^{\tilde{t}_N} \left(\tilde{X}_{s,k}\right)^2 d\tilde{t} \tag{19b}$$

$$\tilde{C}^+_{\varepsilon\varepsilon} = \frac{1}{S\tilde{T}^2_{max}\,\tilde{t}_N} \sum_{s=1}^{S} \int_0^{\tilde{t}_N} \left(\tilde{X}_{s,\varepsilon}\right)^2 d\tilde{t} \tag{19c}$$

$$\tilde{C}^+_{k\varepsilon} = \frac{1}{S\tilde{T}^2_{max}\,\tilde{t}_N} \sum_{s=1}^{S} \int_0^{\tilde{t}_N} \tilde{X}_{s,k}\,\tilde{X}_{s,\varepsilon}\, d\tilde{t} \tag{19d}$$

Also, S stands for the number of temperature sensors used, $\tilde{t}_{\mathrm{N}}$ is the dimensionless duration of the experiment ($\tilde{t}_N = N\,\Delta\tilde{t}$), $\tilde{X}_{s,\gamma}$ (with γ=k, ε) are the dimensionless scaled sensitivity coefficients evaluated at the s-th sensor location, while $\tilde{T}_{\max}$ is the maximum dimensionless temperature reached during the experiment at the corner $\tilde{x} = 0$, $\tilde{y} = 0$.

Note also that, by defining the dimensionless coefficients as shown in Eqs. (19b)-(19d), the determinant Δ^+ is unchanged in value if more than one sensor is placed at the same location.

It is worth noting that the Δ^+ determinant for the 2D problem depends on seven decision variables: the heating and experiment times ($\tilde{t}_{\mathrm{h}}$ and $\tilde{t}_{\mathrm{N}}$), the location of the sensor (x and y coordinates), the number of the sensors (S), the width of the heated region ($\tilde{W}_0$) and the aspect ratio of the sample ($\tilde{W}$), as suggested by the functional dependence of the coefficients defined by Eqs. (19b)-(19d) appearing in Eq. (19a) for the Δ^+. All the variables listed before have been investigated in the design of the optimal experiment with the only exception of the aspect ratio which has been kept constant in the analysis.

5.1. Expected standard deviations

The expected standard deviations related to the optimal experiment aimed at estimating k and ε , simultaneously, can be computed through the covariance matrix of the estimates [19] which in dimensionless form can be taken as

$$\begin{bmatrix} \tilde{\sigma}^2_k & \tilde{\sigma}_{k,\varepsilon} \\ \tilde{\sigma}_{\varepsilon,k} & \tilde{\sigma}^2_\varepsilon \end{bmatrix} = \frac{1}{\Delta^+} \begin{bmatrix} \tilde{C}^+_{\varepsilon\varepsilon} & -\tilde{C}^+_{k\varepsilon} \\ -\tilde{C}^+_{\varepsilon k} & \tilde{C}^+_{kk} \end{bmatrix} \tag{20a}$$

where the determinant Δ^+ and the coefficients $\tilde{C}^+_{kk}$, $\tilde{C}^+_{\varepsilon\varepsilon}$ and $\tilde{C}^+_{\varepsilon k}=\tilde{C}^+_{k\varepsilon}$ are defined by Eqs. (19a)-(19d). Also, the dimensionless standard deviations of k and ε result in

$$\tilde{\sigma}^+_k=\frac{\sigma_k}{k}\frac{\left(T_{\max}-T_{in}\right)\sqrt{N}}{\sigma}\cong\sqrt{\frac{\tilde{C}^+_{\varepsilon\varepsilon}}{\Delta^+}} \tag{20b}$$

$$\tilde{\sigma}^+_\varepsilon=\frac{\sigma_\varepsilon}{\varepsilon}\frac{\left(T_{\max}-T_{in}\right)\sqrt{N}}{\sigma}\cong\sqrt{\frac{\tilde{C}^+_{kk}}{\Delta^+}} \tag{20c}$$

Note that in the above equations σ denotes the standard deviation of the measurement error.

6. Results and discussion

In this section the experimental devices sketched in figures 1a (uniform heating) and 1b (partial heating) are compared in terms of their optimal experiments aimed at estimating k and ε. These optimal experiments are designed by maximizing the Δ^+ determinant defined by Eq. (19a) with respect to two experimental variables: 1) the dimensionless duration of the heating $\tilde{t}_h$ and 2) the dimensionless duration of the experiment $\tilde{t}_N$. In detail, this determinant has to be plotted as a function of $\tilde{t}_N$ with $\tilde{t}_h$ as a parameter, as shown for instance by Figure 5 obtained when using a single sensor at ($\tilde{x}=0$, $\tilde{y}=0$). This figure highlights that the optimal $\tilde{t}_N$ is the time for which the maximum Δ^+ determinant occurs, while the curve that yields the maximum of the maximum Δ^+ values defines the optimal $\tilde{t}_h$.

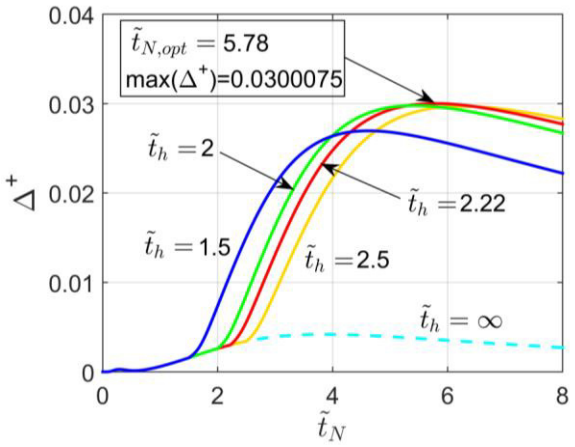

Figure 5. Δ^+ determinant as a function of the experiment duration $\tilde{t}_N$ with the heating duration $\tilde{t}_h$ as a parameter, when using one sensor at the corner ($\tilde{x}=0$, $\tilde{y}=0$).

It is worth noting that when a uniform heating is applied to the samples (1D X22B50T0 problem), only two non-embedded sensors locations can be considered, that is, the front-side ($\tilde{x}=0$) and the back-side ($\tilde{x}=1$) of the sample; on the contrary when a piecewise-uniform heating is applied, several non-embedded sensors locations are possible along the y direction, as the heat diffusion is two-dimensional. Therefore, for the latter case (X22B(y5t5)0Y22B00T0 problem) the optimal experiment is designed for six different sensors configurations, each of which involves one or more temperature sensors placed in different locations along the y direction. These sensors locations are here denoted as

$\tilde{y}_{1s}$, $\tilde{y}_{2s}$ … where the subscripts "1s", "2s" are referred to the first sensor, or the second one and so on. The six temperature sensors configurations here investigated are discussed afterwards in the following order: a) one sensor (S=1) at $\tilde{x}=0$, b) two sensors (S=2) at $\tilde{x}=0$, c) three sensors (S=3) at $\tilde{x}=0$, d) four sensors (S=4) at $\tilde{x}=0$, e) one sensor at $\tilde{x}=0$ and another at $\tilde{x}=1$, f) two sensors at $\tilde{x}=0$ and other two at $\tilde{x}=1$.

6.1. One sensor at the front side

A comparison between the case of partial heating and that of uniform heating, when using a single temperature sensor at $\tilde{x}=0$, is provided by figure 6. In particular, the Δ^+ determinant and the optimal experiment duration $\tilde{t}_{N,\mathrm{opt}}$ are plotted as a function of the sensor location, with the dimensionless width of the heated region W_0/L as a parameter, in figures 6a and 6b, respectively.

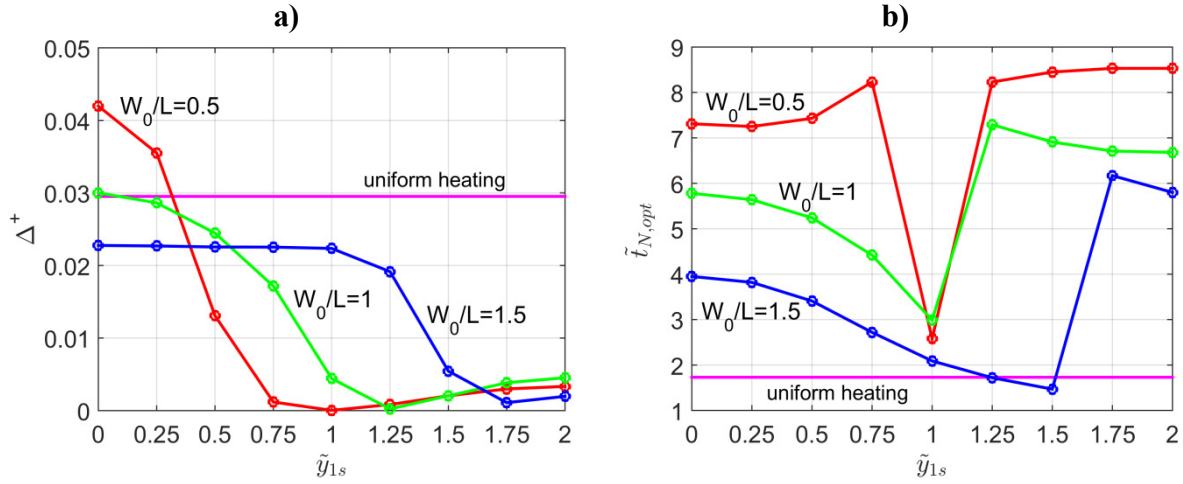

Figure 6. OED when using one sensor at $\tilde{x}=0$: a) Δ^+ determinant and b) optimal experiment duration as a function of the sensor location with W_0/L as a parameter.

From figure 6a one can observe that the partial heating yields small values of the Δ^+ determinant when compared to those obtained when a uniform heating is applied, except for a narrow heated region (W_0/L<1) provide that the temperature sensor is placed near to y=0. However, in such a case a much longer experiment is required as shown by figure 6b. For instance, using a single sensor located at ($\tilde{x}=0$, $\tilde{y}=0$) for a 2.5 cm-thick stainless steel sample (k=40 W/(mK); ε=380 J/(m^{2}Ks$^{1/2}$)) the optimum experiment should have a duration of about 97 s under a uniform heating, while it should be about four times longer (t_N=411 s) when the same sample is tested using the partially heated set-up. Consequently, the perfect insulated condition at the sample backside is not strictly valid anymore and, therefore, the heat loss through the insulating material has to be considered as discussed in Section 3. On the other hand, the high number of measurements recorded during a longer experiment may yield greater computational efforts in the evaluation of the sensitivity matrix involved in the estimation procedure, see Eqs. (8a)-(8b), as its dimensions increases as shown by Eq. (9a). In fact, for example, using two sensors (i.e., S=2) its dimensions are 1940x2 when performing the shorter experiment (t_N=97 s), while it is a 8220x2 matrix in the longer experiment (t_N=411 s).

Moreover, as shown by figure 6a each Δ^+ curve exhibits a minimum value (close to zero) at a specific sensor location. This is due to high correlation between parameters k and ε occurring at that location and for that particular experimental set-up. Note also that, the minimum value of the Δ^+ determinant is reached with a short experiment duration for a small heated region (W_0/L=0.5), while for wider heated regions it occurs for a longer experiment time (see figure 6b).

6.2. Two sensors at the front side

The results obtained when using two sensors at the surface $\tilde{x} = 0$ for the X22B(y5t5)0Y22B00T0 case are displayed in figures 7 and 8. In detail figure 7 shows the Δ^+ determinant as a function of the second sensor location $\tilde{y}_{2s}$ with the location of the first sensor $\tilde{y}_{1s}$ as a parameter, and for different values of the dimensionless width of the heated region W_0/L; while figure 8 shows the corresponding optimal experiment durations. In both figures a comparison with the optimal experiment obtained when using a uniform heating is also given. It is worth noting that when the locations of the two sensors are equal to each other ($\tilde{y}_{1s} = \tilde{y}_{2s}$), Eqs. (19a)-(19d) yield the same results obtained for a single sensor (marked points with black diamonds in figures 7 and 8).

As shown by figure 7 the highest values of the Δ^+ determinant are obtained when the heating is applied over a small region of the sample front-side (W_0/L=0.5). Note that in such a case when placing the first sensor at $\tilde{y}_{1s} = 0$ or $\tilde{y}_{1s} = 0.25$, the partial heating may yield determinant values higher than that obtained through a uniform heating (see figure 7a). However, figure 8a suggests that in such a case the optimal duration of an experiment performed by applying the partial heating is longer than that required when a uniform heating is applied.

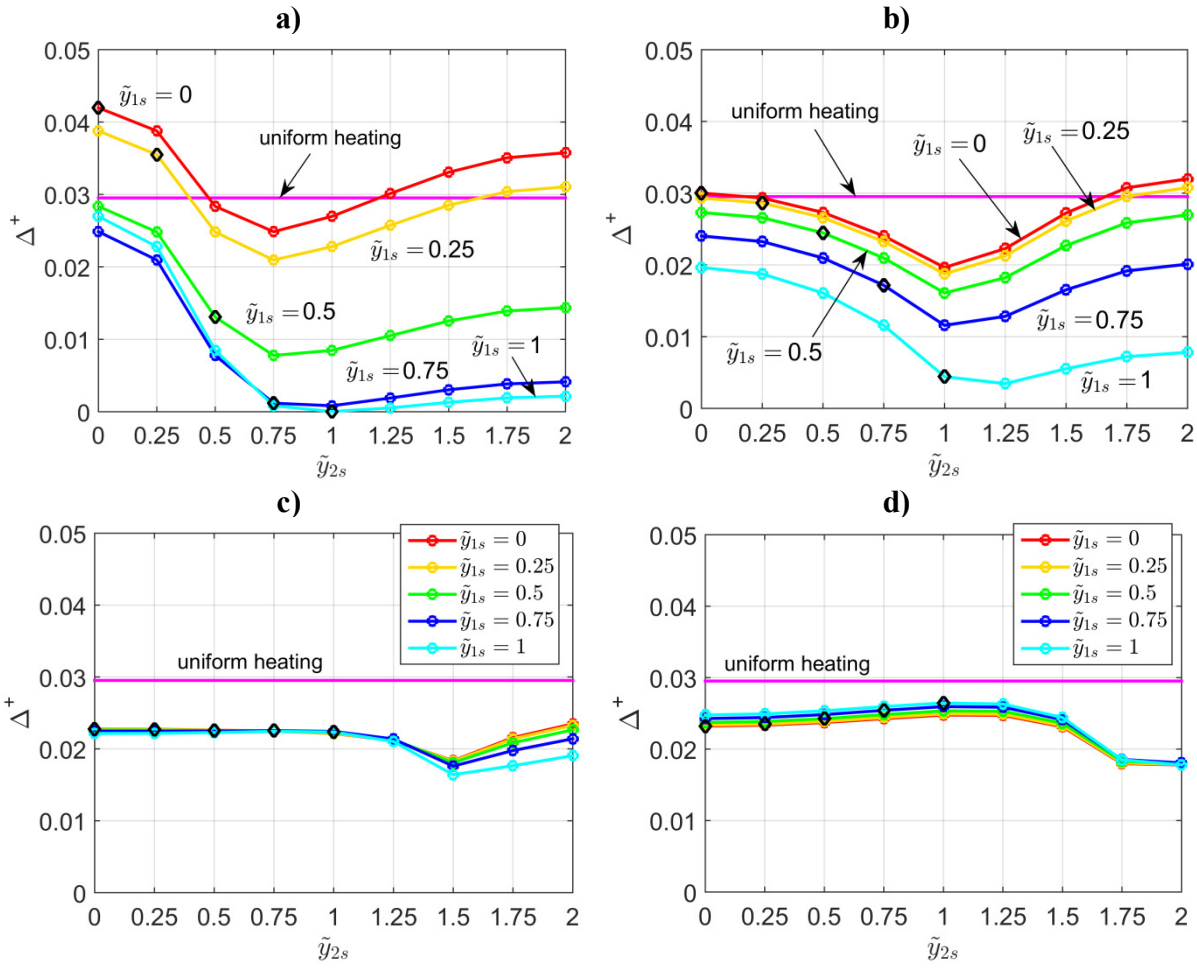

Figure 7. Δ^+ determinant when using two sensors at $\tilde{x} = 0$ for: a) W_0/L=0.5; b) W_0/L=1; c) W_0/L=1.5; d) W_0/L=1.75

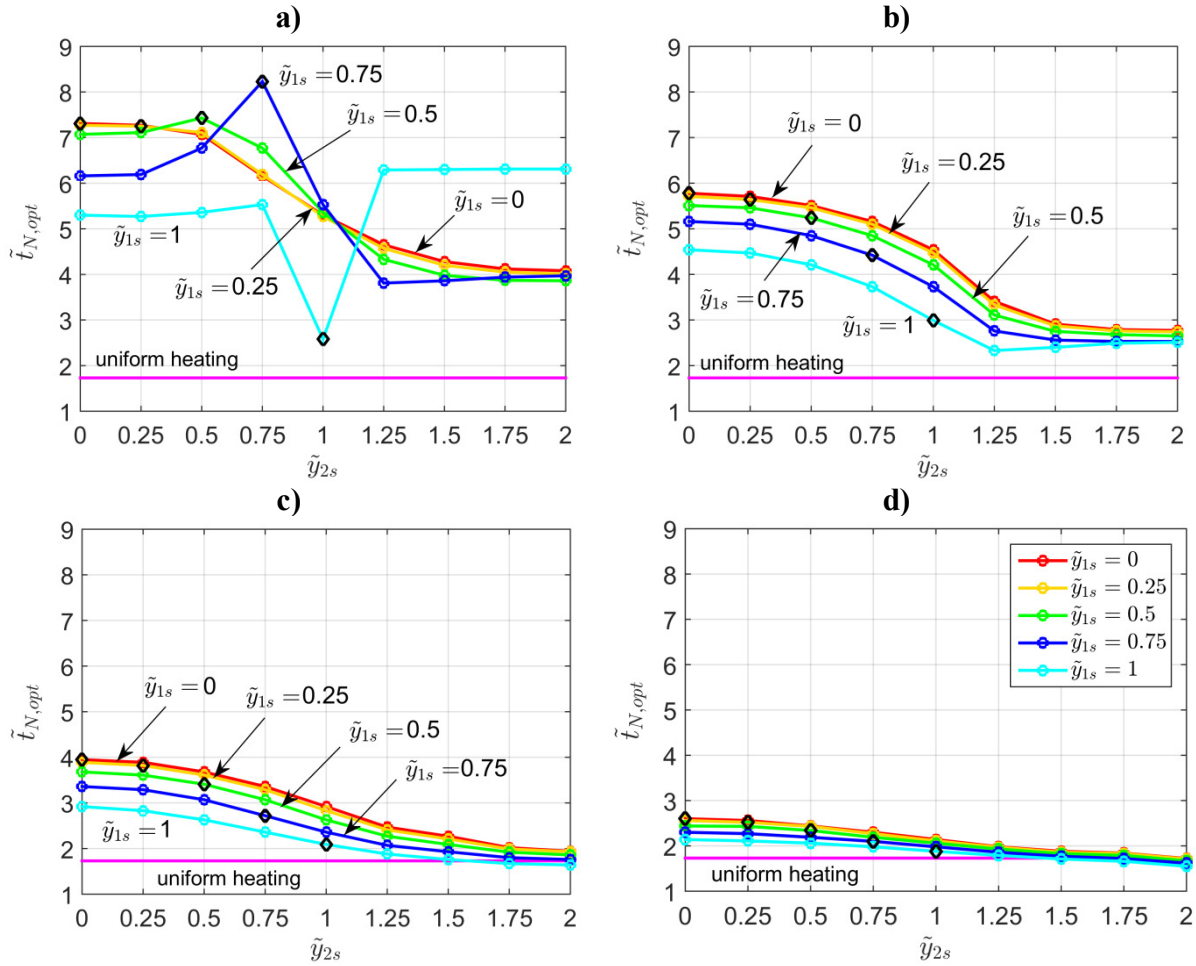

Figure 8. Optimal experiment duration when using two sensors at $\tilde{x}=0$ for:
a) W_0/L=0.5; b) W_0/L=1; c) W_0/L=1.5; d) W_0/L=1.75

6.3. Three sensors at the front side

The case of three temperature sensors placed on the surface $\tilde{x}=0$ has been investigated by considering several combinations of sensors, in which the first of them is placed at $\tilde{y}_{1s}$ =0.25, 0.5 or 0.75. Also, the optimal experiment has been designed for different set-ups of the experimental apparatus i.e., for different values of W_0/L (0.5, 1, 1.5 or 1.75). For the sake of brevity, figure 9 shows only the highest values of the Δ^+ determinant obtained through the best set-ups and the best sensors configurations, together with the related optimal experiment duration. Similarly to the previous figures a comparison with the optimal experiment obtained when applying a uniform heating is also given. As shown by figures 9a, 9c and 9e when using three sensors at the sample front-side, the Δ^+ determinant is lower than or equal to that obtained when using one sensor at $\tilde{x}=0$ under a uniform heating. In particular, the two cases offer the same determinant only when the three sensors are placed at $\tilde{y}_{1s}$ =0.25, $\tilde{y}_{2s}$=0.5, $\tilde{y}_{3s}$=2 , respectively (see figure 9a); however, in such a case the optimal experiment duration is almost doubled compared to the uniform heating case, as shown by figure 9b.

Note that when two of the three sensors are placed in the same location along y (i.e, $\tilde{y}_{1s}=\tilde{y}_{2s}$, $\tilde{y}_{1s}=\tilde{y}_{3s}$ or $\tilde{y}_{2s}=\tilde{y}_{3s}$), the case of three sensors at $\tilde{x}=0$ simply reduces to the case of two sensors discussed in Subsection 6.2 (marked points with black diamonds in figure 9).

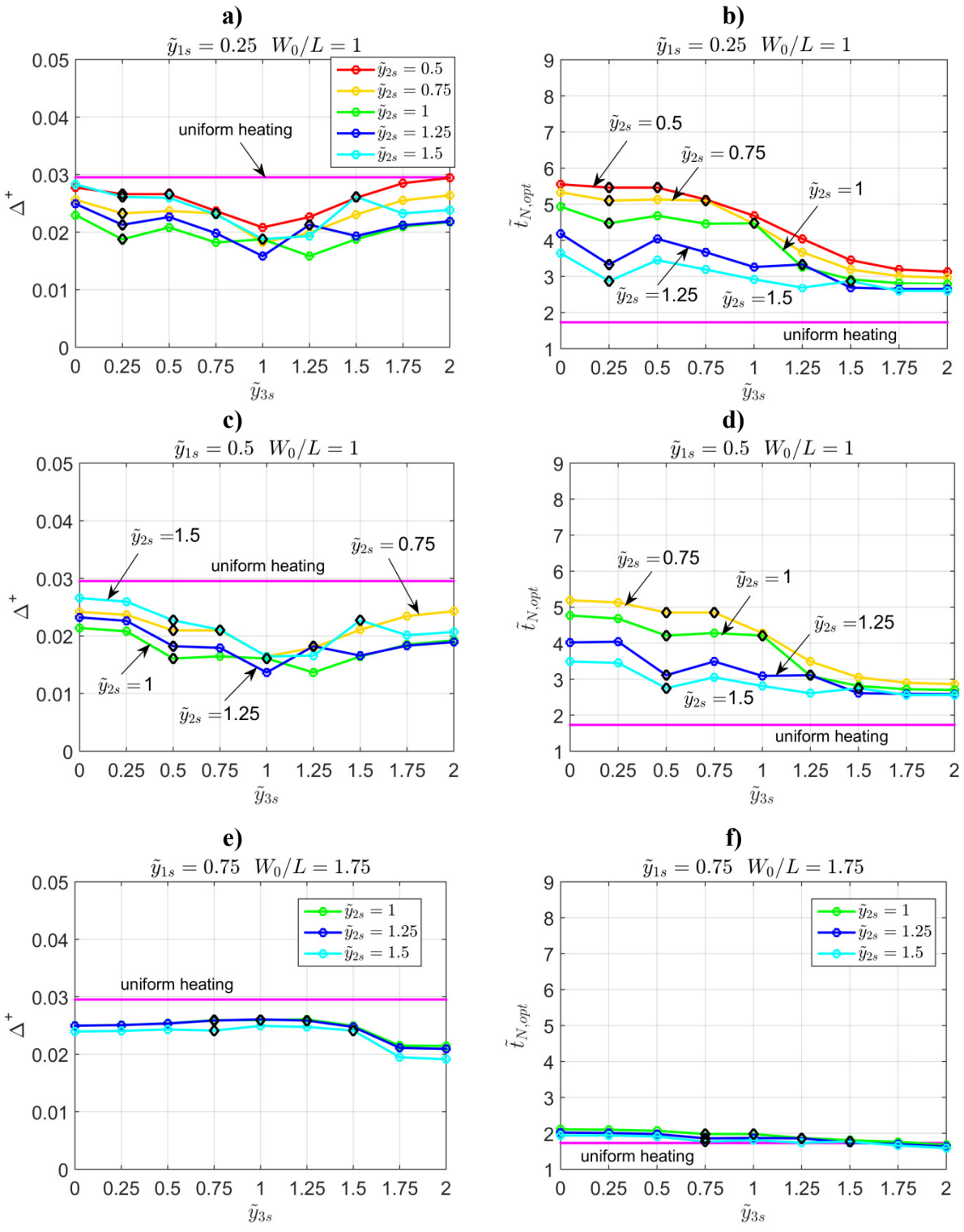

Figure 9. Δ^+ determinant and $\tilde{t}_{N,\mathrm{opt}}$ when using three sensors at $\tilde{x} = 0$ as a function of the third sensor location $\tilde{y}_{3s}$ with the second one location $\tilde{y}_{2s}$ as a parameter and for the best set-up: $\tilde{y}_{1s}$ =0.25 and W_0/L =1 a), b); $\tilde{y}_{1s}$ =0.5 and W_0/L =1 c), d); $\tilde{y}_{1s}$ =0.75 and W_0/L =1.75 e), f).

6.4. Four sensors at the front-side

Due to the large number of possible combinations of four sensors placed at the sample front-side, it is very hard to investigate all of them exhaustively. For this reason table 1 shows the Δ^+ determinant obtained for only some of the most promising combinations (those having at least one or two sensors inside the heated region). Also, the results are given for different values of the dimensionless width of the heated region W_0/L. Moreover, a immediate comparison with the Δ^+ determinant obtained under a uniform heating (using a single sensor at $\tilde{x} = 0$) is provided in the same table. As shown by the table, the maximum values of the determinant obtained for a partial heating (marked in bold) are always lower than the maximum determinant obtained by applying a uniform heating.

Table 1. Δ^+ determinant for different W_0/L when using four temperature sensors.

Sensors locations y/L	max(Δ^+)			uniform heating (X22B50T0)
	W_0/L=0.5	W_0/L =1	W_0/L =1.5	
0.25 0.5 1.25 1.5	0.01963232	0.02213908	0.01986298	
0.25 0.5 1.5 1.75	**0.02166560**	**0.02612014**	0.01972143	
0.25 0.5 1.25 1.75	0.02047604	0.02387740	0.02162392	
0.25 0.75 1.25 1.5	0.01623455	0.01948726	0.01978438	
0.25 0.75 1.5 1.75	0.01795938	0.02315573	0.01935369	
0.25 0.75 1.25 1.75	0.01696826	0.02111908	0.02143736	
0.5 0.75 1.25 1.5	0.00741827	0.01773193	0.01977084	max(Δ^+)
0.5 0.75 1.5 1.75	0.00876020	0.02121005	0.01916393	0.02952076
0.5 0.75 1.25 1.75	0.00800837	0.01929711	0.02135320	
0.25 0.5 0.75 1.25	0.01640470	0.02119326	0.02185144	
0.25 0.5 0.75 1.5	0.01760903	0.02359511	0.02079110	
0.25 0.5 0.75 1.75	0.01846043	0.02543525	0.02277554	
0.25 0.5 0.75 2	0.01876577	0.02611063	**0.02386860**	
0.25 1.25 1.5 1.75	0.01867953	0.01774965	0.01705180	

6.5. One sensor at $\tilde{x} = 0$ and another at $\tilde{x} = 1$

The case of one sensor placed at the sample front side and the other one at the sample backside is now discussed. Several sensor configurations have been tested: in each of them the location of the sensor at $\tilde{x} = 0$ is fixed, while the location of the sensor placed at the sample backside is varied. In particular, five different locations are considered along the y direction that is, y=0, 0.5, 1, 1.5 and 2.

In figures 10a-10c the results obtained using the Δ^+ criterion are plotted as a function of the dimensionless width of the heated region, when the sensor placed at the front side is located at $\tilde{y}_{1s}$ =0, 0.5 and 1, respectively. Note that these are the positions yielding the highest determinant values. In fact, by comparing figures 10a-10c it is evident that to increase the Δ^+ determinant it is needed to locate the front sensor inside the heated region.

Then, from each of these graphs the better sensors collocation has been defined as that that yield the highest Δ^+ determinant, with an optimal experiment duration as brief as possible. The better sensors configurations resulting from this analysis are compared to each other in figure 11, in terms of determinant (figure 11a) and $\tilde{t}_{N,\mathrm{opt}}$ (figure 11b). In both figures 10 and 11 a comparison with the results obtained by applying a uniform heating (using one sensor at $\tilde{x} = 0$ and another one at $\tilde{x} = 1$) is also provided. By observing figure 11a it is possible to state that the partial heating yields Δ^+ determinant values lower than that obtained under a uniform heating. An exception is the case in which the front sensor is placed at $\tilde{y}_{1s}$ =0 and the rear sensor at $\tilde{y}_{1s}$ =2, with a narrow heated region ($\tilde{W}_0 < 0.5$). However, in such a case from one hand the increasing of the Δ^+ determinant is very limited (see figure 11a), but on the other hand the related experiment should be more than four times longer than the optimal one required applying a uniform heating, as shown by figure 11b.

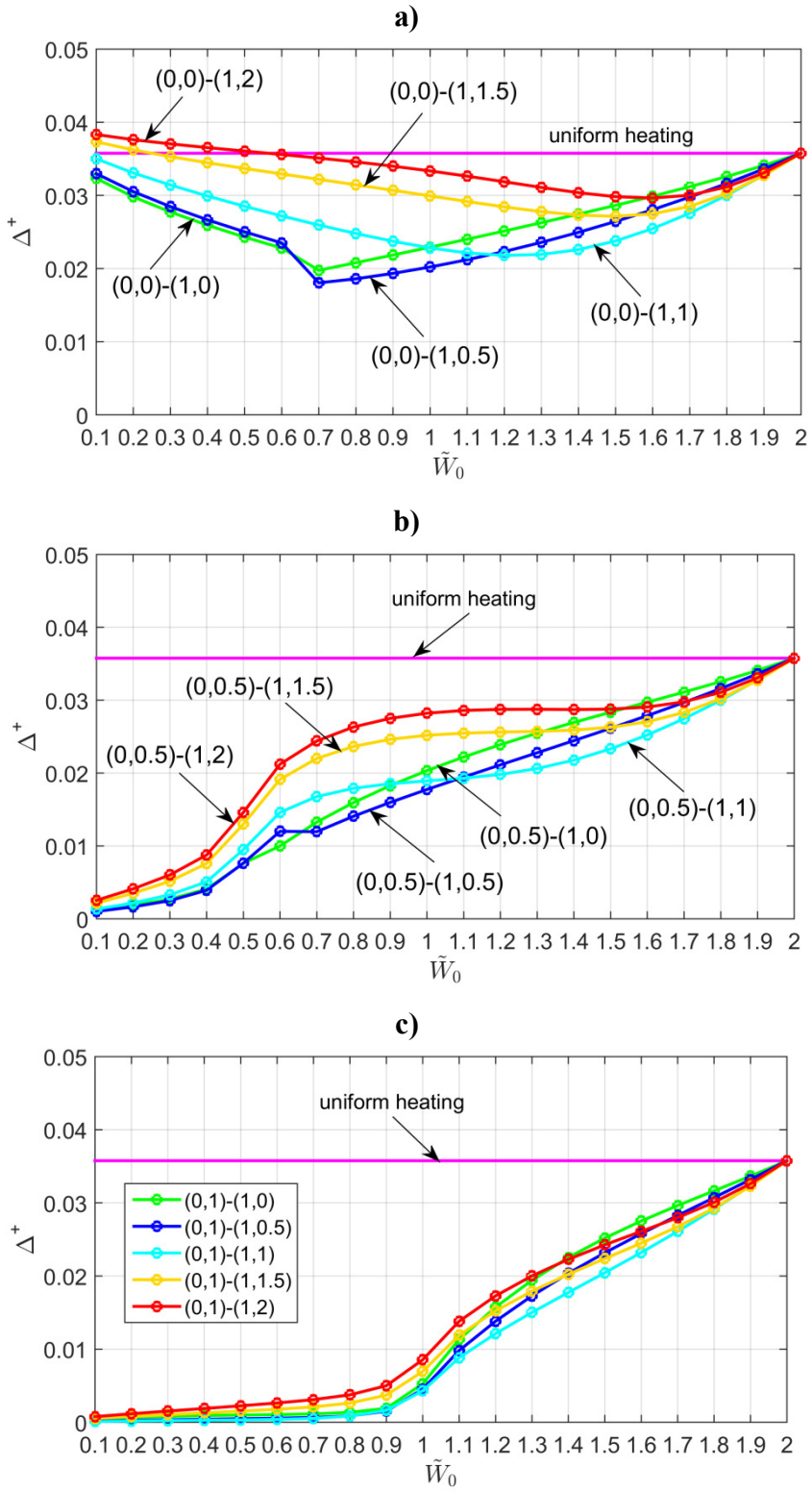

Figure 10. Δ^+ determinant when using two sensors: the former at $\tilde{x} = 0$ located at $\tilde{y}_{1s}$ =0 a), $\tilde{y}_{1s}$ =0.5 b) and $\tilde{y}_{1s}$ =1 c), and the latter placed at $\tilde{x} = 1$ in different positions along the *y*-direction.

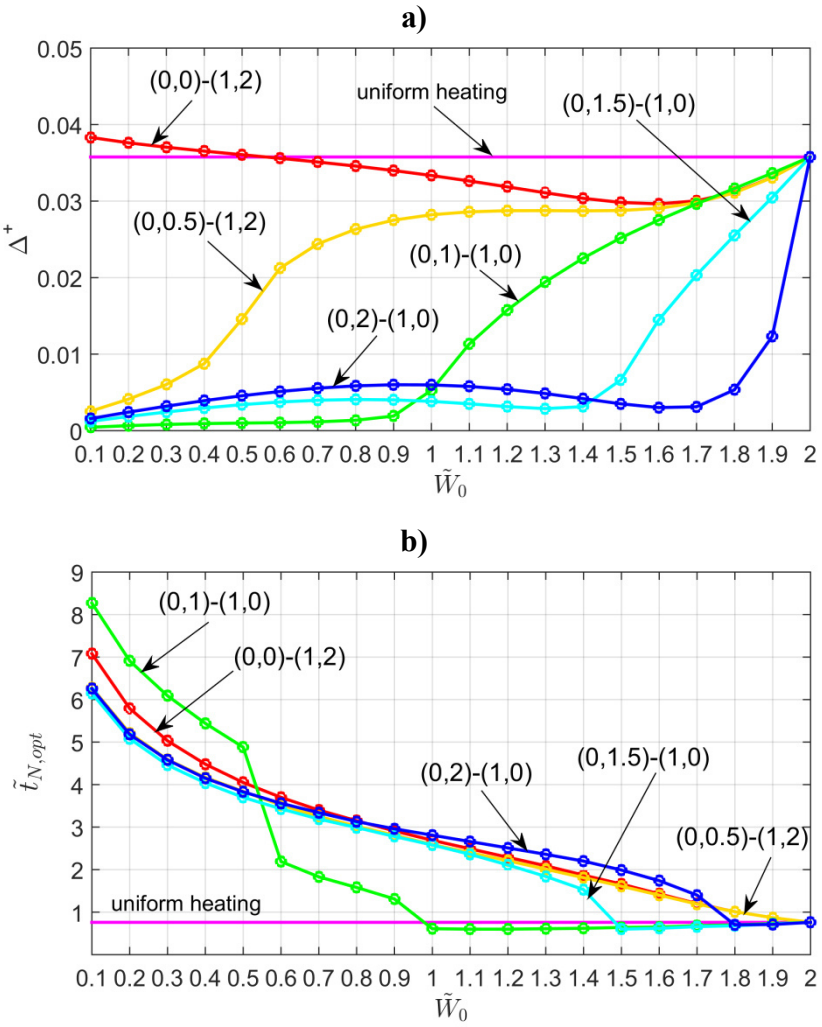

Figure 11. Comparison among the better sensors configurations when using one sensor at the front side and another one at the backside of the sample: a) Δ^+ determinant, and b) optimal experiment duration.

6.6. Two sensors at $\tilde{x}=0$ and two at $\tilde{x}=1$

The last studied case is that involving two sensors at the front side and other two at the sample backside. Due to the large number of possible combinations, the optimization criterion defined by Eqs. (19a)-(19d) has been applied to several configurations having the couple of front sensors (those placed at $\tilde{x}=0$) located in eight different couples of points. For each of these eight couples, the locations of the other two sensors placed at the sample backside have been varied along the *y*-direction.

The results of this analysis have shown that the highest values of the Δ^+ determinant are obtained when the couple of rear sensors are placed at $\tilde{y}=0.75$ and $\tilde{y}=2$. The Δ^+ determinant and the optimal experiment duration related to the five best sensors configurations as a function of the dimensionless width of the heated region, found as described above, are plotted in figures 12a and 12b, respectively. Similarly to the previous cases, a comparison with the results obtained under a uniform heating (using one sensor at $\tilde{x}=0$ and one at $\tilde{x}=1$) is provided in the same figure. As suggested by figure 12, the partial heating yields Δ^+ determinant values lower than that obtained by applying a uniform heating.

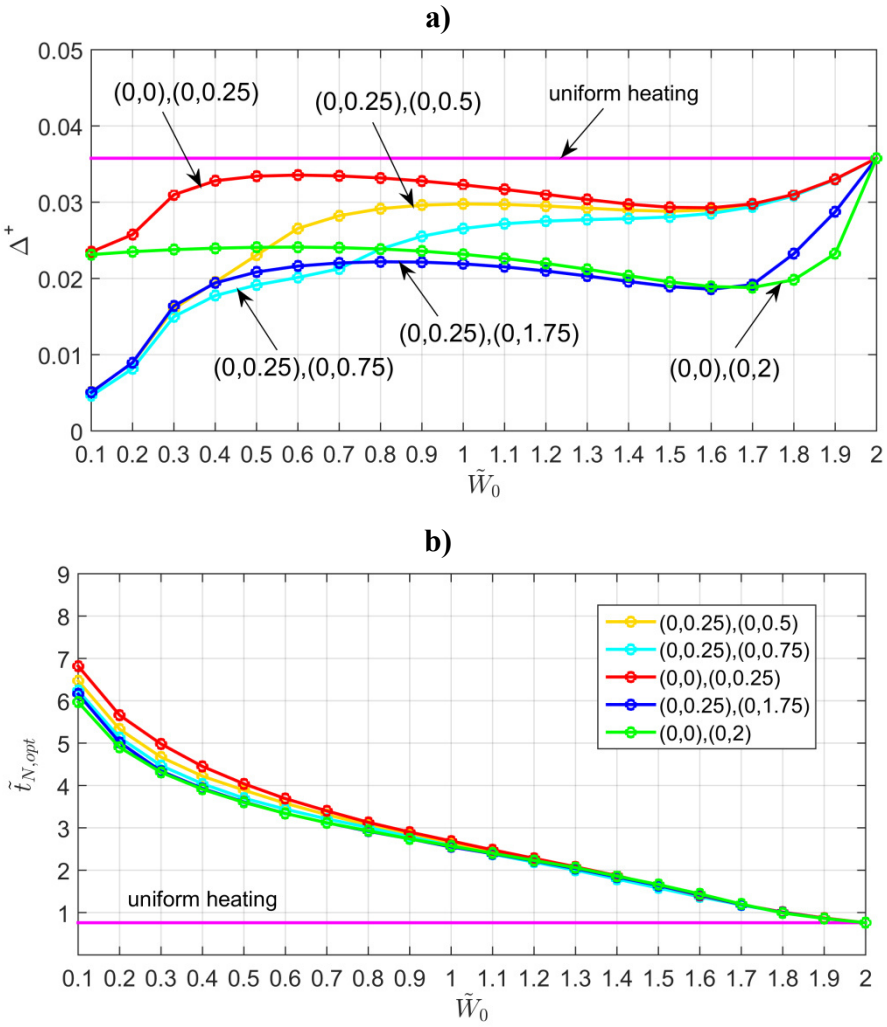

Figure 12. Comparison among the better sensors configurations when using two sensors at the front side and other two located at (1,1.75) and (1,2): a) Δ^+ determinant, and b) optimal experiment duration.

6.7. Expected standard deviations

The expected standard deviations of k and ε when performing the optimal experiment for four sensors configurations are plotted as a function of the dimensionless width of the heated region in figures 13a and 13b, respectively. In detail, the four sensors configurations here considered involve the use of a single sensor at the corner (0,0), a couple of front sensors, one sensor at the front side and another at the sample backside, and four sensors (two at the front side and two at the backside), respectively. For each configuration the optimal experiment designed above, for different values of W_0/L, is used to compute the expected standard deviations through Eqs. (20b) and (20c). Also, a comparison with the standard deviations obtained under a uniform heating using both one sensor at the front side and two sensors (one on the front and one at the rear of the sample) is provided in the same figure.

By observing figure 13 it is evident that the accuracy obtainable for the estimates of k is lower than that expected for the thermal effusivity ε. Although a partial heating may offer a greater accuracy of the estimates of both k and ε especially when using only front sensors, it requires longer experiment times than those required by applying a uniform heating as discussed previously. A small exception is the case of two front sensors located at (0,0) and (0,2) for a dimensionless heated region $1<W_0/L<1.5$.

In fact this experimental set-up would yield a lower $\tilde{\sigma}_k^+$ value and almost the same $\tilde{\sigma}_\varepsilon^+$ obtainable through a uniform heating, but requiring an experiment having approximately the same duration as shown by figures 8b and 8c. However, the corresponding Δ^+ determinant would be less than that obtained under a uniform heating (see figure 7c).

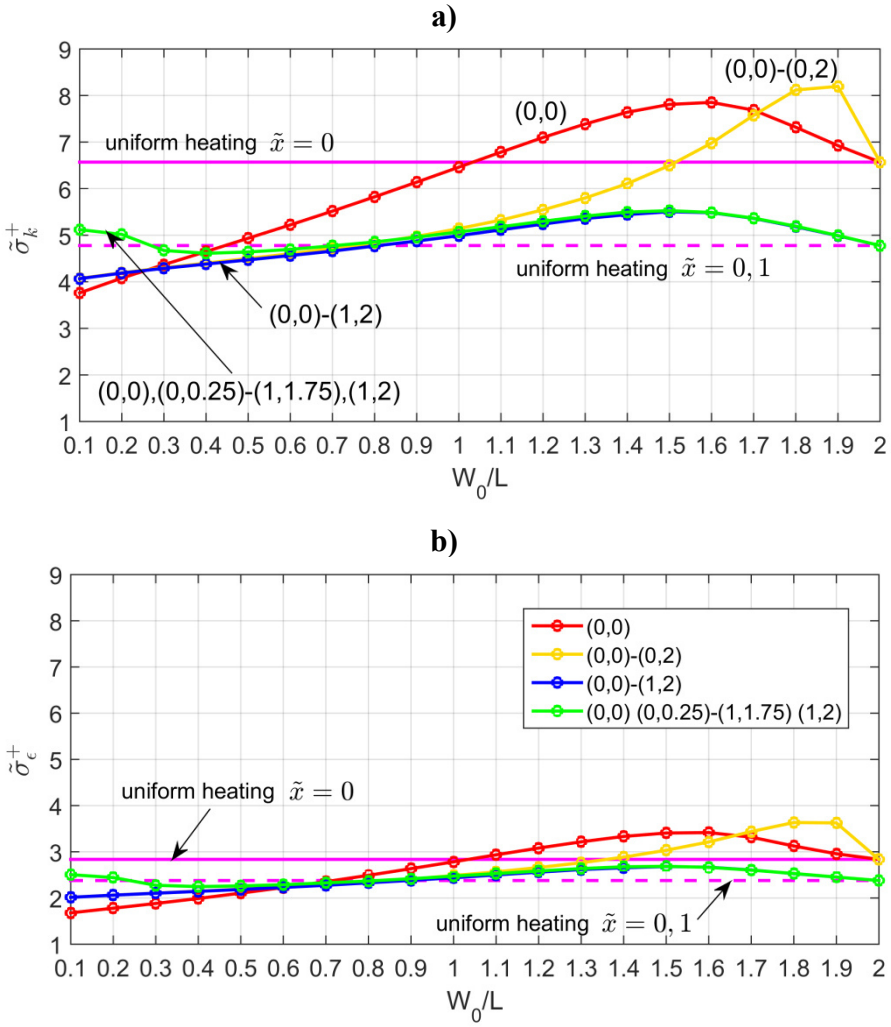

Figure 13. Dimensionless standard deviations related to the optimal experiment for four sensors configurations: a) k, and b) ε.

7. Conclusions

The optimal experiment aimed at estimating k and ε when using the plane source-based experimental apparatus has been designed by applying both a uniform and a piecewise-uniform heating. A D-optimum criterion ensuring a small area of the confidence region of the estimated parameter has been used. The Δ^+ determinant and the related optimal experiment duration obtained for different set-ups and several sensors configurations have been compared in graphical and tabular form. Then the expected standard deviations of k and ε for the best sensors configurations have been also provided. The results of the analysis have shown that the use of a piecewise-uniform heating is not completely beneficial when simultaneously estimating the thermal properties of isotropic materials. In fact, if on

one hand it may offer standard deviations reduced up to about 40% when it is used to estimate k and ε, on the other hand it would require an experiment about four times longer than that required by a uniform heating to ensure a good convergence of the estimation procedure. Therefore, a major computational effort is required.

References

[1] Ahadi M, Andisheh-Tadbir M, Tam M and Bahrami M 2016 An improved transient plane source method for measuring thermal conductivity of thin films: Deconvoluting thermal contact resistance *Int. J. Heat Mass Transfer* **96** 371–380.

[2] Dowding K, Beck J V, Ulbrich A, Blackwell B and Hayes J 1995 Estimation of thermal properties and surface heat flux in carbon-carbon composite *J. Thermophysics Heat Transfer* **9** 2 pp. 345-351.

[3] Hammerschmidt U 2003 A new pulse hot strip sensor for measuring thermal conductivity and thermal diffusivity of solids *Int. J. Thermophysics* **24** 3 pp. 675-682.

[4] Zhang H, Li Y and Tao W 2017 Effect of radiative heat transfer on determining thermal conductivity of semi-transparent materials using transient plane source method *Applied Thermal Eng.* **114** pp. 337-345.

[5] Malheiros F A, Figueiredo A A A, da S. Ignacio L H and Fernandes H C 2019 Estimation of thermal properties using only one surface by means of infrared thermography *Applied Thermal Eng.* **157** 5 113696.

[6] Dowding K J, Beck J V and Blackwell B F 1996 Estimation of directional-dependent thermal properties in a carbon-carbon composite *Int. J. Heat Mass Transf.* **39** 15 3157-3164.

[7] Dowding K J, Blackwell B F and Cochran R J 1998 Application of sensitivity coefficients for heat conduction problems, Sandia Report, Albuquerque, NM, USA, SAND98-0543C.

[8] Aviles-Ramos C and Haji-Sheikh A 2001 Estimation of thermophysical properties of composites using multi-parameter estimation and zeroth-order regularization, *Inverse Prob. Eng.* **9** 507-536.

[9] Mzali F, Sassi L, Jemni A, Ben Nasrallah S and Petit D 2004 Optimal experiment design for the identification of thermo-physical properties of orthotropic solids *Inverse Prob. Sci. Eng.* **12** 193–209.

[10] Rodrigues F A, Orlande H R B and Mejias M M 2004 Use of a single heated surface for the estimation of thermal conductivity components of orthotropic 3D solids *Inverse Prob. Sci. Eng.* **12** 501–517.

[11] de Monte F and Beck J V 2009 Eigen-periodic-in-space surface heating in conduction with application to conductivity measurement of thin films *Int. J. Heat Mass Transf.* **52** 5567–5576.

[12] Malinaric S and Dieska P 2016 Stepwise and pulse transient methods of thermophysical parameters measurement *Int. J. Thermophys.* **37** 12 1–9.

[13] D'Alessandro G and de Monte F 2022 On the optimum experiment and heating times when estimating thermal properties through the plane source method *Heat Transfer Eng.* **43** 257-269.

[14] D'Alessandro G, de Monte F and Amos D E 2019 Effect of heat source and imperfect contact on simultaneous estimation of thermal properties of high conductivity materials *Math. Problems Eng.* **2019** 1–15 Article ID 5945413.

[15] Wouwer A V, Point N, Porteman S and Remy M 2000 An approach to the selection of optimal sensor locations in distributed parameter systems *J Process Control* **10** 291–300.

[16] Berger J, Dutykh D and Mendes N 2017 On the optimal experiment design for heat and moisture parameter estimation *Experimental Thermal and Fluid Science* **81** 109-122.

[17] Taktak R, Beck J V and Scott E P 1993 Optimal experimental design for estimating thermal properties of composite materials *Int. J. Heat Mass Transf.* **36** 12 2977-2986.

[18] D'Alessandro G and de Monte F 2019 Optimal experiment design for thermal property estimation using a boundary condition of the fourth kind with a time limited heating period *Int. J. Heat Mass Transfer* **134** 1268–1282.
[19] Beck J V and Arnold K J 1977 *Parameter Estimation in Engineering and Science* (New York: John Wiley and Sons).
[20] Ucinski D 2005 *Optimal measurement methods for distributed parameter system identification* (CRC Press).
[21] Ruffio E, Saury D and Petit D 2012 Robust experiment design for the estimation of thermophysical parameters using stochastic algorithms *Int. J. Heat Mass Transf.* **55** 2901-2915.
[22] Dieb T M and Tsuda K 2018 *Machine learning-based experimental design in materials science* In *Nanoinformatics*; Tanaka I, Eds.; Springer: Singapore, pp. 65–74.
[23] Wei H, Zhao S, Rong Q and Bao H 2018 Predicting the effective thermal conductivities of composite materials and porous media by machine learning methods *Int. J. Heat Mass Transf.* **127** 908–916.
[24] Gasparin S, Berger J, D'Alessandro G and de Monte F 2022 Optimal experimental design for the assessment of thermophysical properties in existing building walls. In Proceedings of the 10th International Conference on Inverse Problems in Engineering, Francavilla al Mare, Italy, 15-19 May 2022.
[25] Woodbury K A, Najafi H and Beck J V 2017 Exact analytical solution for 2-D transient heat conduction in a rectangle with partial heating on one edge *Int. J. Therm. Sci.* **112** 252-262.
[26] Cole K D, Beck J V, Woodbury A and de Monte F 2014 Intrinsic verification and a heat conduction database *Int. J. Therm. Sci.* **78** 36–47.
[27] McMasters R L, de Monte F and Beck J V 2019 Generalized solution for two-dimensional transient heat conduction problems with partial heating near a corner *ASME J. Heat Transfer* **141** (7) pp. 071301-1 - 071301-8.
[28] Beck J V, Mishra D K and Dolan K D 2017 Utilization of generalized transient heat conduction solutions in parameter estimation in proceedings of the 9th International Conference on Inverse Problems in Engineering ICIPE, Waterloo, Canada, May 23-26 2017.
[29] Cole K D, Beck J V, Haji-Sheikh A and Litkouhi B 2011 *Heat Conduction Using Green's Function 2nd Edition* (Boca Raton FL: CRC Press Taylor&Francis)
[30] McMaster R L, de Monte F and Beck J V 2018 Estimating two heat-conduction parameters from two complementary transient experiments *J. Heat Transfer (ASME)* **140** (7) pp. 071301-1–071301-8.
[31] Blackwell B F, Cochran R J and Dowding K J 1999 Development and implementation of sensitivity coefficient equations for heat conduction problem *Num. Heat Transfer Part B* **36** 15-32.
[32] Mishra D K, Dolan K D, Beck J V and Ozadali F 2017 Use of Scaled Sensitivity Coefficient Relations for Intrinsic Verification of Numerical Codes and Parameter Estimation for Heat Conduction *ASME J. Verification, Validation Uncertainty Quantification* **2** 031005.
[33] Jumabekova A, Berger J, Foucquier A and Dulikravich G S 2020 Searching an optimal experiment observation sequence to estimate the thermal properties of a multilayer wall under real climate conditions *Int. J. Heat Mass Transfer* **155** 119810.